A step forward in the equivalence between thermal and differential-flow modulated comprehensive two-dimensional gas chromatography methods

A step forward in the equivalence between thermal and differential-flow modulated comprehensive two-dimensional gas chromatography methods

Federico Stilo[1], Elena Gabetti[1], Carlo Bicchi[1], Andrea Carretta[2], Daniela Peroni[2], Stephen E. Reichenbach[3,4], Chiara Cordero[1*], James Mc Curry[5]

Authors' affiliation:

1. Università degli Studi di Torino Turin - Italy E-M@il: chiara.cordero@unito.it
2. SRA Intruments SpA, Cernusco sul Naviglio, Milan, Italy
3. University of Nebraska-Lincoln, NE USA
4. GC Image LLC, Lincoln, NE USA
5. Agilent Technologies, Gas Phase Separations Division, Wilmington DE, USA

* Address for correspondence:

Prof. Dr. Chiara Cordero - Dipartimento di Scienza e Tecnologia del Farmaco, Università di Torino, Via Pietro Giuria 9, I-10125 Torino, Italy – e-mail: chiara.cordero@unito.it ; phone: +39 011 6702197

Abstract

Comprehensive two-dimensional gas chromatography (GC×GC) based on flow-modulation (FM) is gaining increasing attention as an alternative to thermal modulation (TM), the recognized GC×GC benchmark, thanks to its lower operational cost and rugged performance. An accessible, rational procedure to perform method translation between the two platforms would be highly valuable to facilitate compatibility and consequently extend the flexibility and applicability of GC×GC. To enable an effective transfer, the methodology needs to ensure preservation of the elution pattern, separation power, and sensitivity.

Here, a loop-type thermal modulation system with dual detection (TM-GC×GC-MSD/FID) used for the targeted analysis of allergens in fragrances is selected as reference method. Initially, six different columns configurations are systematically evaluated for the flow-modulated counterpart. The set up providing the most consistent chromatographic separation (20 m x 0.18 mm d_c x 0.18 µm d_f + 1.8 m x 0.18 mm d_c x 0.18 µm d_f) is further evaluated to assess its overall performance in terms of sensitivity, linearity, accuracy, and pattern reliability. The experimental results convincingly show that the method translation procedure is effective and allows successful transfer of the target template metadata. Additionally, the FM-GC×GC-MSD/FID system is suitable for challenging applications such as the quantitative profiling of complex fragrance materials.

Key-words:

Two-dimensional comprehensive gas chromatography-mass spectrometry and flame ionization detection; reverse-inject differential flow modulation; suspected fragrance allergens; method translation; method limit of detection; repeatability and precision

1. Introduction

Comprehensive two-dimensional gas chromatography GC×GC coupled with mass spectrometry (MS) is a powerful technique for detailed profiling and effective fingerprinting of medium-to-high complexity samples. Thermal modulators implementing cryogenic cooling are widely used and, to date, considered the "gold standard" for GC×GC. The effective in-space band-focusing induced by this modulator results in a peak capacity gain (G_n) that is close to the achievable theoretical limit [1]. At the same time, the signal-to-noise ratio greatly increases resulting in a sensitivity gain of one order of magnitude compared to a conventional 1D-GC analysis. Despite these advantages, thermal modulators have some drawbacks related to hardware and operational costs limiting their widespread adoption in quality control and high-throughput screening.

Differential-flow modulators (FMs), such as those based on the Seeley *et al.* design [2,3], are an interesting alternative to thermal modulators (TMs). Configurations can have an adjustable volume/length accumulation loop, as those proposed by Tranchida *et al.* [4–6]. Large accumulation loop volumes limit the overloading, extends the re-injection period and provides multi-stage dynamics with some benefits on separation power and peak symmetry. The first commercial FM used fixed volume accumulation loop devices obtained with Capillary Flow Technology (CFT) microfluidic plates. They implement both the forward fill/flush (FFF) injection dynamics described by Seeley *et al.* [7] and the reverse fill/flush (RFF) dynamics connoted by a more efficient band re-injection, improved 2D peak widths and symmetry, and effective handling of collection-channel overloading [8–12]. Commercial RFF modulators are available from Agilent Technologies [13] and by Sep-Solve with the FM named Insight™ [14]. More recently, Seeley *et al.* [15] proposed the multi-mode modulator (MMM). This device, as it is engineered in the commercial platforms by LECO (Flux™), enables the adoption of conventional column combinations and carrier gas operational flow in both separation dimensions but is characterized by a low duty cycle.

The growing interest in robust and cryogen-free modulators certainly is driven by the possibility they offer to describe in depth the chemical dimensionality of samples [16] with a relative ease of use and low operational costs. FM gives access to peculiar features of GC×GC separations such as group-type characterization, accurate profiling, and advanced fingerprinting based on 2D separation patterns [17–21]. However, FM dynamics are connoted by a limited flexibility in terms of operative flows in the two separation dimensions which in turn require a careful selection of column dimensions/characteristics to fully exploit the separation potential.

If the price to pay is mainly related to the actual separation power of the system, absolute method sensitivity is another important issue to consider; to date this method characteristic lacks of dedicated research especially in the perspective of application transfer between TM to FM platforms. This study fills this gap by systematically examining six different column combinations, almost equivalent to a reference TM system, for their chromatographic performances and method's figures of merit. Method translation principles [22–25] are here applied for a rational and effective translation of the reference methodology

developed for a loop-type TM system to the six FM tested column configurations, instead of a trial-and-error approach to set chromatographic parameters. By this rational approach, the first-dimension (^{1}D) elution order and resolution of the original TM method are preserved and resulting 2D peak patterns are coherent between mutually translated methods. At the same time, in view of routine applications, analysis speed is also evaluated.

The best performing configuration is then examined for method performance parameters in terms of linearity over a 3 order of magnitude in analytes concentrations, sensitivity and quantitation accuracy. As a challenging application, raw fragrance materials of medium complexity are considered and a selection of targeted analytes referred to as "established contact allergens in humans" by the EU Scientific Committee on Consumer Safety [26] are subjected to quantitative profiling. They included 60 analytes (single compounds or mixtures of isomers) covering a wide range of polarity and volatility.

2. Materials and methods

2.1 Raw materials, pure reference compounds and solvents

Pure standards of *n*-alkanes (from *n*-C9 to *n*-C25) for Linear Retention Indices (I^T) calibration were from Merck (Milan, Italy). Pure standards (or isomers mixtures) of tested analytes listed in **Table 1** were purchased from Merck (Milan, Italy) or kindly provided by Firmenich SA (Geneva, Switzerland). Solvents (cyclohexane and dichloromethane) were all HPLC-grade from Merck (Milan, Italy). Pure standards of 1,4-dibromobenzene and 4,4'- dibromobiphenyl used as Internal Standards (ISTDs) were from Merck (Milan, Italy).

Commercial raw fragrance materials for accuracy assessment were kindly provided by Farotti srl (Rimini, Italy). Test sample #1 (TS1) consisted of a *citrus-like* fragrance while test sample #2 was a *flowery-like* fragrance (TS2).

2.2 Reference solutions and calibration mixtures

Standard Stock Solutions (SS) of reference analytes were prepared at a concentration of 10 mg/mL in dichloromethane or cyclohexane and stored at -18°C. The Model Mixture (MMix) stock solution was prepared by mixing suitable amounts of SS at a final concentration of 200 mg/L in cyclohexane. Fresh calibration solutions were prepared every week by diluting suitable amounts of MMix in cyclohexane. Calibration levels covered were: 0.1-0.2-0.5-1-5-10-20-50-100 mg/L. ISTDs were at a final concentration of 50 mg/L. Standard reference solutions for purity evaluation (by 1D-GC-FID) were prepared from SS at a nominal concentration of 100 mg/L in cyclohexane.

Raw fragrances TS1 and TS2 were diluted 20% (w/v) immediately before analysis in cyclohexane. For accuracy evaluation, spiked samples were prepared by adding suitable volumes of MMix up to +10 mg/L and +1 mg/L concentration levels. ISTDs were added to all analyzed samples at 50 mg/L.

112 **2.3 GC×GC with reverse-inject differential flow modulation: instrument set-up**

113 GC×GC analyses with reverse-inject differential flow modulation were run with a GC-MS system
114 consisting of an Agilent 7890A GC unit provided with a 4513A auto injector sampler (Agilent, Little Falls, DE,
115 USA) and coupled to an Agilent 5977B HES (High Efficiency Source) fast quadrupole MS detector (Agilent,
116 Little Falls, DE, USA) operating in EI mode at 70 eV and a fast FID detector. The GC transfer line was set at
117 280°C. The MS was tuned using the *HES Tune* option. The scan range was set to m/z 40-240 with a scanning
118 rate of 12,500 amu/s to obtain a spectrum generation frequency of 28 Hz. The flame ionization detector (FID)
119 conditions were: base temperature 280°C, H_2 flow 40 mL/min, air flow 350 mL/min, make-up (N_2) 20 mL/min,
120 and sampling frequency 200 Hz.

121 The system was equipped with a reverse-inject FM (Supplementary Material **Figure SF1**) consisting
122 of a CFT plate connected to a three-way solenoid valve that receives a controlled supply of carrier gas
123 (helium) from an auxiliary electronic pressure control module (EPC). The CFT plate schematic and modulation
124 dynamics description are provided in the Supplementary Material (**SF1**).

125

126 **2.4 GC×GC with thermal modulation: instrument set-up**

127 The TM GC×GC system consisted of an Agilent 7890B GC unit with a 4513A auto injector sampler
128 (Agilent, Little Falls, DE, USA) coupled with a Bench TOF-Select™ time of flight mass spectrometer (Markes
129 International, Llantrisant, UK). Electron ionization was set at 70 eV. The ion source and transfer line were set
130 at 290°C. The MS optimization option was set to operate in Single Ionization with a mass range between 35
131 and 550 m/z; data acquisition frequency was 100 Hz; filament voltage was set at 1.60 V. For parallel
132 detection, the FID was set with a base temperature of 280°C, H_2 flow 40 mL/min, air flow 350 mL/min, make-
133 up (N_2) 20 mL/min, and sampling frequency 200 Hz.

134 The system was equipped with a two-stage KT 2004 loop thermal modulator (Zoex Corporation,
135 Houston, TX) cooled with liquid nitrogen controlled by Optimode™ V.2 (SRA Instruments, Cernusco sul
136 Naviglio, MI, Italy). The hot jet pulse time was set at 250 ms, modulation period was 5 s, and cold-jet total
137 flow was progressively reduced with a linear function from 35% of Mass Flow Controller (MFC) at initial
138 conditions to 5% at the end of the run.

139 Injections of the Calibration mixtures (CAL), as well as those for I^T_S determination, were carried out
140 with a 4513A auto injector under the following conditions: injection mode: split, split ratio: 1/20 for CAL and
141 1/50 for *n*-alkanes, injection volume 2 µL, temperature 270°C.

142

2.5 Column set, connections and auxiliary control modules

The reference method (i.e., TM-GC×GC) columns configuration and those tested with FM-GC×GC to achieve comparable method performance are summarized in **Table 2**. Pressure settings (S/SL injector and Auxiliary EPC), carrier gas (helium) volumetric flows in the two dimensions, linear velocities across capillaries, and oven temperature programs also are reported. Calculations were by reference equations and/or by a validated pneumatic model designed for the CFT plate [27].

Connections between the second-dimension (^{2}D) column and deactivated silica capillaries toward MS and FID for parallel detection were by a three-way un-purged splitter (G3181B, Agilent, Little Falls, DE, USA) while columns connection in the TM-GC×GC was by deactivated ultimate unions (G3182-61580 Agilent, Little Falls, DE, USA). ^{1}D columns DB-1, ^{2}D columns OV17 and deactivated capillaries were from Agilent - J&W (Little Falls, DE, USA).

2.6 Performance parameters: reference equations

To evaluate the performances of the tested FM configurations compared to the reference method, several chromatographic performance parameters were considered. The reference parameters and equations are described here.

Re-injection pulse width ($^2\sigma_i$) directly affects the actual $^2\sigma_t$ with an additive effect on ^{2}D peak-broadening due to the chromatographic process ($^2\sigma_c$). Re-injection pulses were defined as peak standard deviation ($^2\sigma_i$) and estimated on un-retained solvent peaks from FID channel (200 Hz sampling frequency) [28].

The net separation measure ($S_{GC\times GC}$) [29] describes system's separation ability under the experimental conditions applied. $S_{GC\times GC}$ extends the concept of separation measure (S) to GC×GC separations [30] and refers to the product of S in each chromatographic dimension:

$$S_{GC\times GC} = S_1 \times S_2 \qquad \textbf{Eq. 1}$$

where S_1 and S_2 are calculated, for ^{1}D and ^{2}D respectively, using the reference equation:

$$S = {\Delta t}/{\sigma_{av}} \qquad \textbf{Eq. 2}$$

where Δt is the arbitrary time interval between two peaks a and b, $\Delta t = t_b - t_a$, and σ_{av} is the peak- standard deviation (σ) of a and b:

$$\sigma_{av} = \frac{(\sigma_a+\sigma_b)}{2} \qquad \textbf{Eq. 3}$$

In this study the time interval was that between the first (i.e., benzaldehyde) and the last (i.e., sclareol) eluting peaks of the MMix for the ^{1}D and the P_M for the ^{2}D.

Pattern coherence was evaluated by relative retention (RR) in the two chromatographic dimensions [11] and taking as reference centroid methyl salicylate and sclareol as last eluting peak. In the ^{2}D the relative retention is normalized to P_M. Here follows reference equations:

177 $^{1}D\ RR = (^{1}D\ Rt_i - {}^{1}D\ Rt_{methyl\ salicylate})/{}^{1}D\ Rt_{sclareol}$ **Eq. 4**

178 $^{2}D\ RR = (^{2}D\ Rt_i - {}^{2}D\ Rt_{methyl\ salicylate})/P_M$ **Eq. 5**

179 Within method performance parameters, linearity in the calibration range (0.1 – 100 mg/L) was
180 evaluated with the determination coefficient of the linear model (R^2) while limits of detection (x_{LOD}) for MS
181 and FID channels were calculated according to EU guidelines [31] as:

182 $$x_{LOD} = 3.9\frac{s_{y,b}}{b}$$ **Eq. 6**

183 where $s_{y,b}$ is the standard deviation of the blank signal and b is the slope of the calibration curve within the
184 lower calibration levels (i.e., 0.1-1 mg/L).

185 Precision was estimated over a one-week validation protocol as repeatability [32] and expressed as
186 percent relative standard deviation (% RSD). It was calculated on retention times in the two dimensions ($^{1}t_R$
187 and $^{2}t_R$) at all calibration points (n=8) and for all analytical replicates (n= 2). Repeatability on absolute and
188 normalized 2D volumes were calculated for the analytical replicates in the middle of the calibration range at
189 1 and 10 mg/L.

190 Accuracy was estimated initially at two spiking levels (i.e., 1 and 10 mg/L in the final sample) and for
191 two commercial fragrances of medium complexity. Bias was expressed as *relative error* % according to the
192 following equation:

193 $$Relative\ error\ \% = \frac{(x_m - x_{exp})}{x_{exp}} \times 100$$ **Eq. 7**

194 where x_m is the estimated amount and x_{exp} is the expected amount after spiking. Accuracy was established
195 analysing TS1 and TS2 samples and spiked ones in triplicate. The *rel. err. %* reported in **Table 1** are those
196 resulting from FID signals except for analytes affected by co-elutions and reported in the table with the
197 symbol "$".

198 **2.7 Data acquisition and 2D data processing**

199 Data were acquired by TOF-DS software (Markes International, Llantrisant, UK) in the reference TM-
200 GC×GC method and Enhanced MassHunter (Agilent Technologies, Little Falls, DE, USA) in the translated FM-
201 GC×GC methods. 2D data were processed by GC Image® GC×GC Edition Software, Release 2.9 (GC Image, LLC
202 Lincoln NE, USA).
203

204 **3. Results and Discussion**

205 **3.1 Background for the present study and reference method**

206 In previous studies, we successfully applied the principles of method translation from a reference
207 method, implemented with a loop-type thermal modulator GC×GC-MS/FID platform, to a reverse-inject
208 differential flow modulated GC×2GC-MS/FID platform [11,12]. The configuration tested in the FM-GC×GC
209 consisted of a ^{1}D with reduced internal diameter and length, compared to the reference set up, and two-
210 parallel ^{2}D columns each one directed to a different detector (MS and FID). The column combination included

a polyethylene glycol (PEG) stationary phase in the ^{1}D and 86% polydimethylsiloxane, 7% phenyl, 7% cyanopropyl in the ^{2}D. Based on the models developed by Blumberg and Klee [22,33], translatable parameters were set to preserve ^{1}D peak elution order, ^{1}D peak capacity, and chromatographic resolution. Temperature programming was therefore modified according to the estimated speed gain and corresponding to the ratio between column void times ($t_{M\text{ref}}$ and $t_{M\text{tr}}$). The operation was supported by the method translation software and available as free application on the web [34].

Results were satisfactory and included a reduction of a factor of 2 for the total analysis time (t_A) of the translated method (32.67 min instead of 65.53 min of the original method) and the preservation of the elution order and of the relative retention in the two chromatographic dimensions (i.e., pattern coherence). Pattern coherence, between mutually translatable methods, enabled effective transfer of metadata from the reference methodology by template matching algorithms [11,12,35].

More recently, Aloisi et al. [36] explored the possibility of defining an equivalent standard column set between TM and FM GC×GC. Their strategy was driven by the choice of two equivalent column sets, in terms of separation power, in consideration of the flow restrictions posed by the two systems. Their set up included a TM platform with a ^{1}D 30 m x 0.25 mm d_c x 0.25 µm d_f and a ^{2}D of 1.5 m x 0.25 mm d_c x 0.25 µm d_f with a delay loop of 1.5 m x 0.18 mm d_c while the FM was with a ^{1}D 20 m x 0.18 d_c x 0.18 µm d_f and a ^{2}D of 5 m x 0.32 d_c x 0.25 µm d_f. The two set-ups provided almost equivalent separation power (referred to the efficiency expressed as number of theoretical plates *N*) and analytes relative retention in the two dimensions. However, the FM method had lower sensitivity because of the compensation for the lower re-injection efficiency of the FM system. The authors report that "… *A sample amount 4 x higher was introduced onto the ^{1}D column in the FM analysis, to compensate for the higher sensitivity of CM (i.e., cryo-modulator)*" [36].

Although the sensitivity drop observed with the FM-GC×2GC-MS/FID set up in translated conditions [12] was less drastic, the FM method did not match TM performances. In the mentioned study [12], cocoa volatiles fingerprinting covered 75 of the 130 targeted peaks (58%) and 450 of the 595 (76%) reliable peak-regions compared to the reference TM procedure.

In this study, to make a step forward in the direction of matching, at the same time, separation power and sensitivity, the RFF FM modulator is tested in its full flexibility by combining three different ^{1}D columns with two ^{2}Ds for a total of 6 configurations. The application context is that of the routine quantification of established volatile allergens in fragrances and the reference method that proposed by Belhassen *et al.* [37]. The system included a loop-type TM, with liquid nitrogen, and a parallel dual-secondary column/dual parallel detection configuration (i.e., TM-GCx2GC-MS/FID). The linearity ranges examined were between 2-100 mg/kg for MS and 100-10,000 mg/kg for FID. Accuracy was good and quantitation bias was below 20% of error for the majority of the analytes (85%) [37].

For this study, the reference TM method adopted for benchmarking FM configurations implied a longer ^{1}D column, compared to that of Belhassen *et al.* [37], (e.g., 60 m × 0.25 mm d_c x 0.25 µm d_f) and a

single ^{2}D of wider diameter (e.g., 1.8 m × 0.18 mm d_c x 0.18 µm d_f). Parallel detection by time of flight mass spectrometry (TOF MS) and FID was obtained by post-column splitting with a passive-tee junction and a flow ratio of about 30:70 (MS/FID) in order to balance the relative sensitivity of the two channels. **Table 2** reports in detail the reference method column configuration, helium carrier flows and linear velocities as they were estimated by reference equations, oven programming and total analysis time (t_A), modulation parameters and operative pressure at the inlet (p_i) at the midpoint between the two dimensions (p_{mid}) and at the tee-union. The TM-GC×GC-TOF MS/FID method was tested for its linearity within 0.1 to 100 mg/L; calibration levels below 1 mg/L were explored because of the industrial needs of a quantitation method able to monitor regulated substances even below the conformity limits. The platform including TOF MS and FID (30:70) enabled to cover this requirement for both channels. In addition, the larger ^{2}D column d_c compensates for the limited loadability of 0.1 mm d_c columns while helping in situations where highly abundant components may overload it to the detriment of both ^{2}D separations and TOF MS ionization efficiency.

Based on the reference method, the six different FM combinations are detailed in **Table 2** (Set-up #1a and b; #2a and b; #3a and b). The rationale for their design was based on limitations due to the modulation dynamics, which requires low carrier flow in the ^{1}D and high flows in the ^{2}D. ^{1}D columns tested were therefore 0.10 mm and 0.18 mm d_c with variable phase ratios to enable higher loadability (e.g., 10 m x 0.10 mm x 0.1 or 0.4 µm d_f). ^{2}D columns were set to afford adequate loadability and efficiency to match with the benchmark peak-capacity. Chromatographic performance parameters were at first examined to evaluate the best configuration. The next section reports experimental results on chromatographic performance in a critical perspective.

3.2 Chromatographic performances of FM-GC×GC-MS/FID in translated conditions

The workflow to translate chromatographic parameters is visualized in the Supplementary Material in **Figure SF2**. In practice, estimated operative pressures at the inlet (p_i) and outlet (p_{out} or p_{mid}) of the ^{1}D column in the reference TM method are input in the calculator and used by the model to translate conditions for the FM method. For the FM configuration, the p_i and p_{out} or p_{aux} are set based on the *a priori* fixed flow conditions in both dimensions. The model calculates the oven temperature programming for the FM method by normalizing it according to the system void time (t_m).

Each modulation period (P_M) was defined after a scouting run with each configuration and evaluating the ^{1}D baseline peak-width (w_b) to obtain a comparable modulation ratio (M_R) for all methods [38].

Results are visualized as pseudocolorized images in **Figure 1** for the MMix at 10 mg/L from the FID signal. The accordance between relative retention in both chromatographic dimensions (i.e., pattern coherence) was evaluated through peaks relative retention against a centroid (methyl salicylate) and the last eluting peak (sclareol) for the ^{1}D and against the P_M for the ^{2}D (**Eq. 4** and **Eq. 5**). Results are visualized in **Supplementary Figure 3** (**SF3**) for all configurations. The reference method, visualized in **Figure 1A**, was

characterized by an average re-injection pulse of 20 ms against an average value of 40 ms for the FM-GC×GC (**Figure 2A**). The average $^{1}\sigma$ for reference peaks (first and last eluting) was 2.34 s with a resulting S_1 of 934 (**Figure 2C** and **2D**). **Supplementary Table 1** (**ST1**) reports $^{1}\sigma$ and $^{2}\sigma$ for all targeted peaks. On the other hand, the best performing set for FM, considering only ^{1}D separation efficiency by $^{1}\sigma$, was Set up #1a the one combining ^{1}D 10 m x 0.1 mm d_c x 0.1 µm d_f with a ^{2}D of 0.18 mm d_c that showed an average $^{1}\sigma$ of 1.85 s. However, the S_1 value of this combination was only 304 (**Figure 2D**) due to the lower capacity factors (k) expressed by this set-up.

Insert Figure 1 here

Conversely, average $^{2}\sigma$ were almost comparable for all FM methods (average value of 0.11 s in **Figure 2E**) and, in turn, even better than those estimated for the reference method (i.e., $^{2}\sigma$ 0.17 s). For this reason, all FM systems had comparable separation power in the ^{2}D (**Figure 2F**) with S_2 values ranging between 23 for the Set up #1a [10 m x 0.1 mm d_c x 0.1 µm d_f + 1.8 m x 0.18 mm d_c x 0.18 µm d_f] and 42 for the Set up #3b [20 m x 0.18 mm d_c x 0.18 µm d_f + 2.5 m x 0.25 mm d_c x 0.25 µm d_f].

Insert Figure 2 here

The best performing approach in terms of separation power (i.e., $S_{GC\times GC}$) was Set up #3a, [20 m x 0.18 mm d_c x 0.18 µm d_f + 1.8 m x 0.18 mm d_c x 0.18 µm d_f], with a $S_{GC\times GC}$ value of 22809 against 27464 (~ 83%) of the TM method and a shorter analysis time (~ 78%).

Based on these premises, the FM-GC×GC-MS/FID set up #3a, consisting of [DB1 of 20 m x 0.18 mm d_c x 0.18 µm d_f + OV17 of 1.8 m x 0.18 mm d_c x 0.18 µm d_f], was selected to proceed with the evaluation of performance parameters in a one-week validation protocol. The next section reports experimental results on linearity, limit of detection (LOD), pattern reliability, and accuracy.

3.3 Method performance parameters of the translated FM-GC×GC-MS/FID

3.3.1 Linearity

The calibration ranges explored for reference and translated methods were designed to span 3 to 4 orders of magnitude of concentrations, as it is in general with natural and synthetic fragrance materials [37,39]. Calibration at low levels, between 0.1 and 1 mg/L, was explored to cover trace amounts for analytes of concern.

The reference method confirmed its good linearity at the MS channel (TIC signal) within both: (a) the 0.1-20 mg/L range with a median R^2 of 0.9983 – mean 0.9980 (min 0.9954 / max 0.9998); and (b) in the full range 0.1-100 mg/L with median R^2 of 0.9942 – mean 0.9902 (min 0.9522 / max 0.9999). Benzaldehyde exhibited the worst performance with R^2 0.9522. Linearity at the FID was satisfactory; the median value for R^2 was 0.9963 – mean 0.9959 (min 0.9949 / max 0.9987) within 0.1-100 mg/L although better performances were registered in the higher calibration range (10-100 mg/L) with R^2 median value of 0.9996 – mean 0.9995 (min 0.9984 / max 0.9999). The reference method mean (red cross mark) and median (red line) are reported

316 in red in the scatter plot of **Figure 3A** showing linearity results. R^2 values calculated on linear regression
317 models for the translated method are reported in **Table 1**.
318 **Insert Figure 3 here**
319 The translated candidate method exhibited very good linearity; it has to be considered that the FM-
320 GC×GC includes a single quadrupole MS with high efficiency source (HES) and actual sampling frequency was
321 lower (i.e., 28 Hz) compared to the TOF MS operating at 100 Hz. Despite these configuration differences, the
322 qMS data was highly satisfactory, with results visualized in the scatter diagrams of **Figure 3A**. Median R^2 value
323 for the MS TIC signal was 0.9967 – mean 0.9957 (median – green line / mean – green mark) with a min of
324 0.9850 for hexadecanolactone and a max of 0.9994 for eugenyl acetate in the range 0.1-20 mg/L. Conversely,
325 FID in the full range (0.1-100 mg/L), had median value for R^2 of 0.9972 – mean 0.9964 (median – green line /
326 mean – green mark) with a min of 0.9784 for damascenone delta and a max of 0.9995 for
327 dimethylbenzylcarbinyl acetate (DMBCA).
328 Results indicate that, in terms of linearity within the examined ranges, FM-GC×GC-MS/FID has
329 performances comparable to the reference method. The FID channel has indeed better linear models
330 although, as it will be discussed in the next section, absolute sensitivity for this channel is slightly lower.
331 *3.3.2 Limit of detection*
332 Absolute sensitivity was estimated according to the EU guidelines for food and feed [31], generally
333 more restrictive than those for other fields of application (**Eq. 6**). Results are reported as histograms in **Figure**
334 **4** for FID (**Figure 4A**) and MS (**Figure 4B**). On average, the MS detection channel had higher sensitivity: the
335 mean LOD value of the reference method was 7.25 µg/L, with a maximum value for sclareol (i.e., 29.5 µg/L)
336 and a minimum for limonene (i.e., 2.93 µg/L). The translated method followed exactly the same trend with
337 slightly higher LODs (+ 1.4%). To note: the two platforms were equipped with different MS systems,
338 consequently this data should be read in light of linearity performances. However, if one considers the FM-
339 GC×GC as a suitable system for routine controls, reliability in the established conditions are not affected by
340 the slower acquisition frequency of the qMS.
341 **Insert Figure 4 here**
342 In accordance to MS results, the FID channel sensitivity with the FM-GC×GC was perfectly comparable
343 to that of the TM-GC×GC, revealing an average LOD of 6.36 µg/L *vs.* 6.25 µg/L of the TM (+ 1%).
344 LODs also inform about the relative sensitivity of the two detectors (i.e., MS and FID) and, at the
345 same time, confirm that TIC MS exceeds FID of a factor of 2.3. Of course, by selecting diagnostic ion traces,
346 MS can be even more sensitive and, at the same time, more flexible enabling to overcome co-elution issues.
347 The next section examines pattern reliability, through retention times precision and responses
348 stability.
349 *3.3.3 Repeatability: retention times and responses*
350 Retention time stability is a fundamental characteristic for GC×GC separations, since a primary

criterion for analytes identification is their position in the 2D pattern. **Table 1** reports precision data, expressed as RSD % on ${}^{1}t_R$ and ${}^{2}t_R$ calculated over 8 calibration points and 2 analytical replicates each (n=16 runs). Along the ^{1}D, absolute retention times for the FM method were highly similar showing a RSD % of 0.12. Slightly higher values were obtained for ^{2}D retention, with a RSD% of 0.98. To note, retention of analytes with ^{2}D tailing and/or distortion effects is less precise; linalool resulted in a 1.55 RSD % while vanillin and α-amylcinnamaldehyde had RSD% of 1.40 and 1.68 respectively.

Responses were indeed highly stable; for the FID channel, absolute 2D volumes registered an average precision of 3.51 % (RSD) while normalized values (over respective ISTDs) were on average 2.71%. The TIC MS signal was comparable with RSD% of 3.30 and 3.20 for absolute and normalized responses, respectively.

The next section briefly presents accuracy data on medium complexity fragrances spiked at 1 and 10 mg/L levels.

3.3.4 Accuracy: medium complexity fragrance mixtures

Accuracy was preliminarily assessed for targeted analytes spiked in commercial raw fragrances at 1 and 10 mg/L concentration levels. Bias was expressed as *relative error %* (**Eq. 7**) and calculated on the FID signal. In case of co-elutions, the TIC-MS data were adopted and indicated in Table with the symbol "$". Results are reported in **Table 1** and visualized as scatter plots in **Figure 3B**. Supplementary Figure **SF4** shows pseudocolorized chromatographic images of raw commercial fragrances spiked at 1 and 10 mg/L together with targeted peaks template (coloured circles) and connection lines for ISTDs.

The *relative error* at the higher spiking level (i.e., + 10 mg/L) was lower for *flowery-like* TS2 sample with a median of 6.16 %, calculated on absolute values, compared to the 8.82% at the lower level (i.e., + 1 mg/L). For the *citrus-like* TS1 sample, median values were 7.53% (+ 10 mg/L) and 5.8% (+ 1 mg/L). Minimum and maximum error values were always below ±30%. Results are in line with those validated for the same analytes in the reference method [37], and indicate that the translated FM-GC×GC-MS/FID method is a good candidate for a routine quantification of targeted analytes in medium complexity fragrances.

4. Conclusions

This study evidences the flexibility of RFF FM-GC×GC while suggesting a rational approach to translate chromatographic conditions by keeping coherent separation patterns and avoiding chromatographic distortions (overloading of the accumulation loop, generation of asymmetrical 2D peaks etc.). Moreover, the method translation enables the operator to obtain a separation power in line with a reference methodology with TM-GC×GC and, thanks to a rational procedure, to exploit the flexibility by acting on column characteristics that have direct impact on re-injection efficiency and analysis time.

The best FM configuration, when tested for performances of interest in the context of quantitative profiling, demonstrated linearity, sensitivity, and accuracy comparable to the TM counterpart. However, the need for higher flows to the ^{2}D of a FM system, at least to achieve adequate separation power, slightly limits system performances resulting either in an equivalent separation power at the cost of sensitivity [33] or in a sensitivity and quantitation consistency at the cost of ~20 % separation power.

Acknowledgments

The project was supported by Agilent Applications and Core Technology University Research (ACT/UR) programme. Project #4294 “Development and Validation of Novel Tools to Facilitate Conversion of Thermal Modulated GC×GC Methods to Reverse Flow Modulated GC×GC Methods”

References

[1] M.S. Klee, J. Cochran, M. Merrick, L.M. Blumberg, Evaluation of conditions of comprehensive two-dimensional gas chromatography that yield a near-theoretical maximum in peak capacity gain, J. Chromatogr. A. 1383 (2015) 151–159. doi:10.1016/j.chroma.2015.01.031.

[2] J. V. Seeley, N.J. Micyus, S. V. Bandurski, S.K. Seeley, J.D. McCurry, Microfluidic deans switch for comprehensive two-dimensional gas chromatography, Anal. Chem. 79 (2007) 1840–1847. doi:10.1021/ac061881g.

[3] J. V. Seeley, S.K. Seeley, Multidimensional gas chromatography: Fundamental advances and new applications, Anal. Chem. 85 (2013) 557–578. doi:10.1021/ac303195u.

[4] P.Q. Tranchida, F.A. Franchina, P. Dugo, L. Mondello, Flow-modulation low-pressure comprehensive two-dimensional gas chromatography, J. Chromatogr. A. 1372 (2014) 236–244. doi:10.1016/j.chroma.2014.10.097.

[5] P.Q. Tranchida, F.A. Franchina, P. Dugo, L. Mondello, Use of greatly-reduced gas flows in flow-modulated comprehensive two-dimensional gas chromatography-mass spectrometry, J. Chromatogr. A. 1359 (2014) 271–276. doi:10.1016/j.chroma.2014.07.054.

[6] P.Q. Tranchida, M. Maimone, F.A. Franchina, T.R. Bjerk, C.A. Zini, G. Purcaro, L. Mondello, Four-stage (low-)flow modulation comprehensive gas chromatography-quadrupole mass spectrometry for the determination of recently-highlighted cosmetic allergens, J. Chromatogr. A. 1439 (2016) 144–151. doi:10.1016/j.chroma.2015.12.002.

[7] P.A. Bueno, J. V. Seeley, Flow-switching device for comprehensive two-dimensional gas chromatography, in: J. Chromatogr. A, 2004: pp. 3–10. doi:10.1016/j.chroma.2003.10.033.

[8] J.F. Griffith, W.L. Winniford, K. Sun, R. Edam, J.C. Luong, A reversed-flow differential flow modulator for comprehensive two-dimensional gas chromatography, J. Chromatogr. A. 1226 (2012) 116–123. doi:10.1016/j.chroma.2011.11.036.

[9] C. Duhamel, P. Cardinael, V. Peulon-Agasse, R. Firor, L. Pascaud, G. Semard-Jousset, P. Giusti, V. Livadaris, Comparison of cryogenic and differential flow (forward and reverse fill/flush) modulators and applications to the analysis of heavy petroleum cuts by high-temperature comprehensive gas chromatography, J. Chromatogr. A. 1387 (2015) 95–103. doi:10.1016/j.chroma.2015.01.095.

[10] C. Cordero, P. Rubiolo, L. Cobelli, G. Stani, A. Miliazza, M. Giardina, R. Firor, C. Bicchi, Potential of the reversed-inject differential flow modulator for comprehensive two-dimensional gas chromatography in the quantitative profiling and fingerprinting of essential oils of different complexity, J. Chromatogr. A. 1417 (2015) 79–95. doi:10.1016/j.chroma.2015.09.027.

[11] C. Cordero, P. Rubiolo, S.E. Reichenbach, A. Carretta, L. Cobelli, M. Giardina, C. Bicchi, Method translation and full metadata transfer from thermal to differential flow modulated comprehensive two dimensional gas chromatography: Profiling of suspected fragrance allergens, J. Chromatogr. A. 1480 (2017) 70–82. doi:10.1016/j.chroma.2016.12.011.

[12] F. Magagna, E. Liberto, S.E. Reichenbach, Q. Tao, A. Carretta, L. Cobelli, M. Giardina, C. Bicchi, C. Cordero, Advanced fingerprinting of high-quality cocoa: Challenges in transferring methods from thermal to differential-flow modulated comprehensive two dimensional gas chromatography, J. Chromatogr. A. 1536 (2018) 122–136. doi:10.1016/j.chroma.2017.07.014.

[13] Agilent Reverse-Inject modulator, (n.d.). https://www.agilent.com/cs/library/technicaloverviews/public/technicaloverview-gcxgc-reversed-flow-modulator-5994-0157en-agilent.pdf.

[14] SepSolve Flow Modulator, (n.d.). http://www.sepsolve.com/gcgc-applications/.

[15] J. V. Seeley, N.E. Schimmel, S.K. Seeley, The multi-mode modulator: A versatile fluidic device for two-dimensional gas chromatography, J. Chromatogr. A. 1536 (2018) 6–15. doi:10.1016/j.chroma.2017.06.030.

[16] J.C. Giddings, Sample dimensionality: A predictor of order-disorder in component peak distribution in multidimensional separation, J. Chromatogr. A. 703 (1995) 3–15. doi:10.1016/0021-9673(95)00249-M.

[17] S.E. Reichenbach, X. Tian, C. Cordero, Q. Tao, Features for non-targeted cross-sample analysis with comprehensive two-dimensional chromatography, J. Chromatogr. A. 1226 (2012) 140–148.

446 doi:10.1016/j.chroma.2011.07.046.
447 [18] C. Cordero, E. Liberto, C. Bicchi, P. Rubiolo, S.E. Reichenbach, X. Tian, Q. Tao, Targeted and non-
448 targeted approaches for complex natural sample profiling by GC×GC-qMS, J. Chromatogr. Sci. 48
449 (2010) 251–261. doi:10.1093/chromsci/48.4.251.
450 [19] J. Kiefl, C. Cordero, L. Nicolotti, P. Schieberle, S.E. Reichenbach, C. Bicchi, Performance evaluation of
451 non-targeted peak-based cross-sample analysis for comprehensive two-dimensional gas
452 chromatography-mass spectrometry data and application to processed hazelnut profiling, J.
453 Chromatogr. A. 1243 (2012) 81–90. doi:10.1016/j.chroma.2012.04.048.
454 [20] G. Purcaro, C. Cordero, E. Liberto, C. Bicchi, L.S. Conte, Toward a definition of blueprint of virgin olive
455 oil by comprehensive two-dimensional gas chromatography, J. Chromatogr. A. 1334 (2014) 101–111.
456 doi:10.1016/j.chroma.2014.01.067.
457 [21] F. Magagna, L. Valverde-Som, C. Ruíz-Samblás, L. Cuadros-Rodríguez, S.E. Reichenbach, C. Bicchi, C.
458 Cordero, Combined untargeted and targeted fingerprinting with comprehensive two-dimensional
459 chromatography for volatiles and ripening indicators in olive oil, Anal. Chim. Acta. 936 (2016) 245–
460 258. doi:10.1016/j.aca.2016.07.005.
461 [22] M.S. Klee, L.M. Blumberg, Theoretical and Practical Aspects of Fast Gas Chromatography and Method
462 Translation, J. Chromatogr. Sci. 40 (2002) 234–247. doi:10.1093/chromsci/40.5.234.
463 [23] L.M. Blumberg, Theory of fast capillary gas chromatography. Part 1: Column efficiency, J. High Resolut.
464 Chromatogr. 20 (1997) 597–604. doi:10.1002/jhrc.1240201106.
465 [24] L.M. Blumberg, Theory of fast capillary gas chromatography part. 2: Speed of analysis, J. High Resolut.
466 Chromatogr. 20 (1997) 679–687. doi:10.1002/jhrc.1240201212.
467 [25] L.M. Blumberg, Theory of fast capillary gas chromatography - Part 3: Column performance vs. gas flow
468 rate, HRC J. High Resolut. Chromatogr. 22 (1999) 403–413. doi:10.1002/(SICI)1521-
469 4168(19990701)22:7<403::AID-JHRC403>3.0.CO;2-R.
470 [26] SCCP (Scientific Committee on Consumer Products), Opinion on Fragrance allergens in cosmetic
471 products, Eur. Comm. (2011) 1–136. doi:10.2773/ISBN.
472 [27] M. Giardina, J.D. McCurry, P. Cardinael, G. Semard-Jousset, C. Cordero, C. Bicchi, Development and
473 validation of a pneumatic model for the reversed-flow differential flow modulator for comprehensive
474 two-dimensional gas chromatography, J. Chromatogr. A. 1577 (2018) 72–81.
475 doi:10.1016/j.chroma.2018.09.022.
476 [28] M.S. Klee, J. Cochran, M. Merrick, L.M. Blumberg, Evaluation of conditions of comprehensive two-
477 dimensional gas chromatography that yield a near-theoretical maximum in peak capacity gain, J.
478 Chromatogr. A. 1383 (2015) 151–159. doi:10.1016/j.chroma.2015.01.031.
479 [29] L.M. Blumberg, M.S. Klee, Metrics of separation in chromatography, J. Chromatogr. A. 933 (2001) 1–
480 11. doi:10.1016/S0021-9673(01)01256-0.
481 [30] L.M. Blumberg, Comprehensive two-dimensional gas chromatography: Metrics, potentials, limits, in:
482 J. Chromatogr. A, 2003: pp. 29–38. doi:10.1016/S0021-9673(02)01416-4.
483 [31] T. Wenzl, J. Haedrich, A. Schaechtele, P. Robouch, J. Stroka, Guidance Document on the Estimation of
484 LOD and LOQ for Measurements in the Field of Contaminants in Feed and Food. EUR 28099 EN, 2016.
485 doi:10.2787/8931.
486 [32] Eurachem, Eurachem Guide: The Fitness for Purpose of Analytical Methods – A Laboratory Guide to
487 Method Validation and Related Topics., 2014. doi:978-91-87461-59-0.
488 [33] L.M. Blumberg, M.S. Klee, Optimal Heating Rate in Gas Chromatography, J. Microcolumn Sep. 12
489 (2000) 508–514. doi:10.1002/1520-667X(2000)12:9<508::AID-MCS5>3.0.CO;2-Y.
490 [34] Agilent Method Translation software, (n.d.). https://www.agilent.com/en/support/gas-
491 chromatography/gcmethodtranslation.
492 [35] D.W. Rempe, S.E. Reichenbach, Q. Tao, C. Cordero, W.E. Rathbun, C.A. Zini, Effectiveness of Global,
493 Low-Degree Polynomial Transformations for GCxGC Data Alignment, Anal. Chem. 88 (2016) 10028–
494 10035. doi:10.1021/acs.analchem.6b02254.
495 [36] I. Aloisi, T. Schena, B. Giocastro, M. Zoccali, P.Q. Tranchida, E.B. Caramão, L. Mondello, Towards the
496 determination of an equivalent standard column set between cryogenic and flow-modulated
497 comprehensive two-dimensional gas chromatography, Anal. Chim. Acta. 1105 (2020) 231–236.

498 doi:10.1016/j.aca.2020.01.040.
499 [37] E. Belhassen, D. Bressanello, P. Merle, E. Raynaud, C. Bicchi, A. Chaintreau, C. Cordero, Routine
500 quantification of 54 allergens in fragrances using comprehensive two-dimensional gas
501 chromatography-quadrupole mass spectrometry with dual parallel secondary columns. Part I:
502 Method development, Flavour Fragr. J. 33 (2018) 63–74. doi:10.1002/ffj.3416.
503 [38] W. Khummueng, J. Harynuk, P.J. Marriott, Modulation ratio in comprehensive two-dimensional gas
504 chromatography, Anal. Chem. 78 (2006) 4578–4587. doi:10.1021/ac052270b.
505 [39] A. Chaintreau, E. Cicchetti, N. David, A. Earls, P. Gimeno, B. Grimaud, D. Joulain, N. Kupfermann, G.
506 Kuropka, F. Saltron, C. Schippa, Collaborative validation of the quantification method for suspected
507 allergens and test of an automated data treatment, J. Chromatogr. A. 1218 (2011) 7869–7877.
508 doi:10.1016/j.chroma.2011.08.072.
509
510

Figure Captions:

Figure 1: MMix calibration solution at 10 mg/L analyzed with the different configurations. (**1A**) reference TM-GC×GC-TOFMS/FID; (**1B**) **–** FM Set-up #1a [DB1 10 m × 0.10 mm d_c x 0.10 µm d_f + OV17 1.8 m × 0.18 mm d_c x 0.18 µm d_f]; (**1C**) – FM Set-up #1b [DB1 10 m × 0.10 mm d_c x 0.10 µm d_f + OV17 2.5 m × 0.25 mm d_c x 0.25 µm d_f]; (**1D**) – FM Set-up #2a [DB1 10 m × 0.10 mm d_c x 0.40 µm d_f + OV17 1.8 m × 0.18 mm d_c x 0.18 µm d_f]; (**1E**) – FM Set-up #2b [DB1 10 m × 0.10 mm d_c x 0.40 µm d_f + OV17 2.5 m × 0.25 mm d_c x 0.25 µm d_f]; (**1F**) FM Set-up #3a [DB1 20 m × 0.18 mm d_c x 0.18 µm d_f + OV17 1.8 m × 0.18 mm d_c x 0.18 µm d_f]; (**1G**) – FM Set-up #3b [DB1 20 m × 0.18 mm d_c x 0.18 µm d_f + OV17 2.5 m × 0.25 mm d_c x 0.25 µm d_f].

Figure 2: separation performances for the reference TM-GC×GC-TOFMS/FID method (red bars) compared to translated FM- GC×GC-MS/FID set-up (#1a and b – grey; #2a and b blue; #3a and b green). Performances refer to (**1A**) re-injection pulse width ($^{i}\sigma$); (**1B**) net separation measure ($S_{GC\times GC}$); (**1C**) ^{1}D peak-width expressed as standard deviation ($^{1}\sigma$); (**1D**) ^{1}D separation measure (S_1); (**1E**) ^{2}D peak-width expressed as standard deviation ($^{2}\sigma$); (**1F**) ^{2}D separation measure (S_2).

Figure 3: (**3A**) scatter diagram referring of linearity of calibration models (coefficient of determination R^2) obtained with the FM-GC×GC-MS/FID method and set-up #3a; red marks report mean and median of the reference methodology. (**3B**) shows accuracy results for the two tested raw materials spiked at 1 and 10 mg/L level. Accuracy is reported as relative error % - see section 2.6 for details.

Figure 4: Histograms showing LOD values (µg/L) estimated for the TM- GC×GC-TOFMS/FID (reference – red bars) and FM-GC×GC-MS/FID method and set-up #3a (green bars) on FID signal (**4A**) and TIC MS signal (**4B**).

Table Captions:

Table 1: List of analytes included in the MMix together with FM-GC×GC-MS/FID precision data on ^{1}D and ^{2}D retention times ($^{1}t_R$ and $^{2}t_R$), 2D peak absolute volumes and normalized volumes on FID and MS channels; linearity (R^2) and accuracy (relative error %) at two spiking levels. "$" refers to accuracy data calculated on the TIC-MS signal instead of FID.

Table 2: Reference and translated methods settings, including: columns characteristics, initial head-pressure (p_i), helium volumetric flows, and hold-up times on the basis of reference equations. Oven temperature programming and total analysis time (t_A) are also reported. Operative conditions include also modulation parameters.

Table 1

	Precision - Repeatability										Linearity		Accuracy – *Relative error %*			
	^{1}D Retention (^1t_R)			*^{2}D Retention (^2t_R)*			*FID –Responses %RSD*		*MS TIC – Responses %RSD*				*Citrus-like TS1*		*Flowery-like TS2*	
Compound Name	**min**	**Stdev**	**%RSD**	**sec**	**Stdev**	**%RSD**	**Volumes**	**Norm. Vol.**	**Volumes**	**Norm. Vol.**	**R^2 FID**	**R^2 MS**	**+1 mg/L**	**+10 mg/L**	**+1 mg/L**	**+10 mg/L**
1,4-Dibromobenzene	15.17	0.08	0.50	1.35	0.03	1.87	3.69	0.00	2.55	0.00	-	-	-	-	-	-
4,4'-Dibromobiphenyl	33.55	0.00	0.00	2.00	0.00	0.25	3.57	0.00	1.68	0.00	-	-	-	-	-	-
Benzaldehyde	8.70	0.00	0.00	1.21	0.01	0.63	0.45	1.63	2.07	4.39	0.998	0.994	-7.21	-2.27	-15.07	-12.29
α-Pinene	8.80	0.00	0.00	0.38	0.00	0.00	1.21	0.03	2.95	9.66	0.998	0.989	-5.06	-9.36	-0.22	-6.16
β-Pinene	9.85	0.00	0.00	0.51	0.00	0.57	2.02	0.84	0.90	0.07	0.996	0.999	-5.80	3.16	-0.11	-2.75
Benzyl alcohol	10.63	0.03	0.27	1.34	0.02	1.14	0.24	1.42	1.33	1.41	0.998	0.998	15.26	-6.18	-8.44	2.25
α-Terpinene	10.83	0.03	0.27	0.52	0.02	3.87	1.10	0.08	1.40	4.39	0.998	0.997	-21.40	-2.51	12.23	-2.78
Salicylaldehyde	10.88	0.03	0.26	1.34	0.01	0.65	0.70	1.88	3.32	2.60	0.998	0.998	19.74	22.04	-1.86	5.47
Limonene	11.15	0.00	0.00	0.51	0.01	2.03	1.81	0.63	2.59	2.06	0.996	0.990	-6.44	-7.62	-0.87	16.91
Terpinolene	12.75	0.00	0.00	0.64	0.01	1.20	14.58	13.41	2.11	2.91	0.993	0.998	-6.79	-0.10	-7.41	-13.09
Linalool	12.83	0.03	0.22	0.65	0.01	1.55	8.66	9.84	1.81	0.80	0.996	0.996	9.43	-15.61	1.62	-9.05
Camphor	13.95	0.00	0.00	1.13	0.01	0.89	3.24	2.06	0.72	1.10	0.998	0.997	6.39	2.05	-2.60	2.74
Menthol	14.90	0.00	0.00	0.72	0.01	1.44	2.73	1.55	0.69	3.33	0.995	0.996	-8.86	-1.21	-21.80	-0.30
Folione	15.17	0.03	0.19	1.11	0.01	0.45	2.61	1.43	5.63	5.58	0.994	0.997	-9.91	5.22	-6.26	-6.95
Methyl salicylate	15.23	0.03	0.19	1.28	0.01	0.98	2.51	1.33	4.29	4.42	0.997	0.998	-11.74	-0.67	-0.64$^{\$}$	-13.38$^{\$}$
α-Terpineol	15.33	0.03	0.19	0.88	0.01	1.19	3.13	1.95	8.65	1.31	0.997	0.997	-5.16	0.50	-3.82	-13.03
Citronellol	16.27	0.03	0.18	0.72	0.01	1.44	2.10	0.92	3.28	0.33	0.998	0.993	-2.79	-2.75	-8.83	-4.81
Neral	16.47	0.03	0.18	0.97	0.01	0.79	2.63	1.45	3.16	3.96	0.998	0.997	-1.36$^{\$}$	6.28$^{\$}$	-1.59	-5.68
Carvone	16.50	0.00	0.00	1.20	0.01	0.84	1.22	0.04	4.90	6.15	0.998	0.996	-8.43	0.36	0.60	-0.88
Cinnamaldehyde	16.90	0.05	0.30	1.76	0.01	0.72	3.78	2.60	4.32	6.27	0.998	0.997	-4.59	15.87	-6.79	8.98
Geraniol	16.93	0.03	0.17	0.84	0.01	1.19	0.67	0.51	2.82	3.90	0.998	0.995	17.64	7.77	9.97	8.58
Linalyl acetate	17.10	0.00	0.00	0.66	0.02	2.30	2.66	3.84	4.91	1.61	0.998	0.998	17.12	-6.75	-7.48	-1.31
Geranial	17.18	0.03	0.17	0.98	0.01	0.78	2.14	0.96	0.55	0.42	0.998	0.998	-16.86	11.12	-0.58$^{\$}$	-5.43$^{\$}$
Anise alcohol	17.30	0.05	0.29	1.81	0.02	1.12	1.24	2.42	4.67	8.44	0.998	0.995	-9.85	1.08	-13.22	-10.00
Hydroxycitronellal	17.47	0.03	0.17	1.03	0.01	1.28	2.02	0.84	0.51	0.86	0.997	0.997	-1.03	-3.02	-20.49	-3.19
Anethole trans	17.72	0.03	0.16	1.22	0.01	0.71	4.70	3.52	4.78	1.31	0.998	0.998	-8.64	-0.18	-10.81	-6.72
Cinnamyl alcohol	17.97	0.03	0.16	1.67	0.02	0.91	0.73	0.45	1.34	5.23	0.997	0.998	4.06	13.18	-15.09	8.44
DMBCA	18.65	0.00	0.00	1.07	0.01	1.18	1.03	0.15	3.73	1.81	0.999	0.998	5.08	1.92	-20.04	-6.82
Eugenol	19.47	0.03	0.15	1.34	0.01	0.43	3.28	2.10	1.68	4.40	0.998	0.998	0.03	5.80	-11.21	-10.68
Vanillin	20.05	0.05	0.25	2.15	0.03	1.40	11.32	10.15	11.65	1.31	0.997	0.996	15.05	16.41	12.39	4.13
δ-Damascone	20.22	0.03	0.14	0.94	0.00	0.31	11.86	10.69	5.32	4.68	0.978	0.997	0.31	-8.10	-7.76	0.42
Geranyl acetate	20.23	0.03	0.14	0.87	0.03	3.04	7.85	9.02	4.19	0.19	0.996	0.997	-3.15	13.68	16.80	-6.11
β-Damascenone	20.38	0.03	0.14	1.09	0.01	0.80	4.10	2.92	7.46	8.32	0.997	0.997	-4.00	2.41	-14.15	-4.19
α-Damascone	20.65	0.00	0.00	1.01	0.01	1.25	3.70	2.52	0.22	0.47	0.991	0.992	-6.62	-2.16	-11.71	6.89
Coumarin	21.00	0.05	0.24	2.59	0.03	1.16	2.49	1.31	3.93	3.14	0.997	0.994	-9.81	9.51	-12.50	-17.43
Majantol	21.02	0.03	0.14	1.19	0.01	1.11	4.08	2.91	6.62	1.70	0.998	0.995	-4.25	6.74	-7.89	4.30
β-Damascone	21.17	0.03	0.14	1.03	0.01	0.56	3.41	2.23	1.14	5.97	0.998	0.991	-6.38	-5.46	-14.72	-15.45
Isoeugenol (E)	21.75	0.00	0.00	1.43	0.01	0.73	3.17	1.99	3.03	2.75	0.998	0.998	-19.77	9.51	-14.49	3.96
β-Caryophyllene	21.87	0.03	0.13	0.70	0.01	1.43	3.54	2.36	4.12	7.26	0.993	0.996	-6.30	-1.75	-4.24	-1.37
Ebanol (Z isomer)	22.10	0.00	0.00	0.72	0.01	1.40	3.82	2.64	3.99	1.37	0.998	0.998	4.60	3.64	-13.60	-9.55
Ebanol (E isomer)	22.30	0.00	0.00	0.73	0.01	1.73	3.46	2.28	3.19	0.06	0.997	0.998	-2.12	3.69	-16.47	-8.40
Isomethylionone alpha	22.92	0.03	0.13	0.87	0.01	0.58	4.63	3.45	2.25	0.80	0.996	0.997	-4.56	-1.99	-5.61	-1.88

Eugenyl acetate	23.35	0.05	0.21	1.63	0.01	0.31	4.13	2.95	1.13	3.74	0.997	0.999	-9.11	10.74	-7.44	15.63
Lilial	23.67	0.03	0.12	1.19	0.00	0.24	4.18	3.00	2.51	4.43	0.997	0.996	4.33	-0.18	-5.39	-0.46
Propylidene phtalide	24.57	0.03	0.12	1.79	0.01	0.32	2.71	1.53	0.81	2.08	0.998	0.998	-27.26	9.69	-3.70	10.25
Amyl salicylate	24.93	0.03	0.12	1.03	0.01	0.84	0.28	0.90	6.05	2.63	0.995	0.994	-5.19	1.27	-14.88	-8.85
Isoeugenyl acetate	25.38	0.03	0.11	1.65	0.01	0.46	4.20	3.02	5.88	3.67	0.998	0.992	-9.74	13.06	-6.90	-2.71
Amylcinnamaldehyde alpha	26.47	0.03	0.11	1.24	0.02	1.68	0.21	1.39	5.26	5.58	0.984	0.993	-3.74	22.29	3.02	4.89
Lyral (minor isomer)	26.48	0.03	0.11	1.34	0.01	0.65	11.57	10.40	3.63	5.56	0.996	0.999	3.32	-22.34	-9.54	-4.87
Lyral (major isomer)	26.63	0.03	0.11	1.36	0.01	0.85	3.33	2.16	1.08	0.23	0.997	0.996	-11.96$	14.81$	-12.89	5.80
ISO E Super (major isomers)	27.23	0.03	0.11	0.97	0.01	1.07	3.99	2.81	2.33	1.08	0.998	0.996	-12.23	12.79	-10.56	10.33
Amylcinnamyl alcohol alpha	27.28	0.03	0.11	1.24	0.01	1.01	4.08	2.90	3.02	7.75	0.997	0.990	-5.37	10.41	-17.93	1.20
α-Santalol	27.42	0.03	0.11	0.98	0.01	0.51	2.87	1.69	2.28	5.97	0.996	0.994	-4.36	5.60	-23.17	-4.82
Farnesol	28.22	0.03	0.10	0.86	0.00	0.34	0.47	0.71	4.35	4.58	0.997	0.994	-2.05	9.18	5.50	-14.12
β-Santalol	28.25	0.00	0.00	1.07	0.01	1.17	3.50	2.32	6.66	2.70	0.997	0.998	-3.83	15.37	-12.40	-17.09
α-Hexylcinnamaldehyde	28.63	0.03	0.10	1.17	0.01	0.89	4.83	3.65	6.24	0.05	0.998	0.997	1.03	8.23	-9.73	5.06
Benzyl benzoate	28.78	0.03	0.10	1.88	0.01	0.53	5.25	4.07	7.76	3.91	0.997	0.997	-11.89	8.91	-19.23	-1.93
Acetylcedrene	29.48	0.03	0.10	1.08	0.01	0.71	3.93	2.75	0.09	0.60	0.997	0.999	-3.30	7.53	-11.61	6.86
Benzyl salicylate	31.00	0.05	0.16	1.76	0.01	0.59	1.87	3.04	1.32	0.40	0.997	0.997	2.85	12.59	2.01	10.91
Galaxolide (major isomers)	31.50	0.05	0.16	1.22	0.01	0.47	3.38	2.20	1.53	1.61	0.997	0.997	-4.21	10.25	-8.28	13.56
Hexadecanolactone	32.73	0.03	0.09	1.08	0.01	0.71	3.31	2.13	1.64	1.31	0.993	0.985	8.05	12.62	-10.55	2.86
Benzyl cinnamate	35.03	0.03	0.08	1.92	0.01	0.30	3.09	1.91	0.12	5.82	0.997	0.998	-5.41	19.90	-4.13	19.67
Sclareol	37.82	0.03	0.08	1.23	0.00	0.00	1.87	3.05	3.58	11.29	0.998	0.986	0.15	24.33	-8.06	15.02
Average	/	/	0.12	/	/	0.98	3.51	2.71	3.30	3.20	0.996	0.996	-3.07	4.58	-7.44	-0.69

Table 2

	^{1}D	^{2}D	Connections and capillaries	Oven programming	Modulation parameters
Reference method TM-GC×GC-TOFMS/FID	DB1 60 m × 0.25 mm d_c x 0.25 µm d_f He @ 2.0 mL/min - constant flow Initial head-pressure (p_i relative) 254.7 kPa Outlet pressure (p_{mid} absolute) 163.7 kPa Hold-up 3.52 min - Outlet velocity 46.97 cm/s	OV17 1.8 m × 0.18 mm d_c x 0.18 µm d_f He @ 2.0 mL/min - constant flow Initial head-pressure (p_{mid} absolute) 163.7 kPa Hold-up 1.8 sec - Outlet velocity 106.6 cm/s	Loop-capillary deactivated silica: 1.0 m, 0.10 mm d_c MS/FID split ratio 70:30 to MS: 0.7 m, 0.10 mm d_c to FID: 1.1 m, 0.18 mm d_c	60°C(1') to 280°C (10') @ 4°/min t_A= 48.35 min	P_M = 5s hot-jet pulse: 250 ms
Translated methods FM-GC×GC-MS/FID					
Set-up #1a	DB1 10 m × 0.10 mm d_c x 0.10 µm d_f He @ 0.27 mL/min - constant flow Initial head-pressure (p_i relative) 305.27 kPa Outlet pressure (p_{aux} absolute) 278 kPa Hold-up 0.89 min - Outlet velocity 18.80 cm/s	OV17 1.8 m × 0.18 mm d_c x 0.18 µm d_f He @ 8.0 mL/min - constant flow Initial head-pressure (p_{aux} relative) 177 kPa Hold-up 0.6 sec - Outlet velocity 292.57 cm/s	MS/FID split ratio 70:30 to MS: 0.5 m, 0.10 mm d_c to FID: 1.1 m, 0.18 mm d_c bleeding capillary: 6.37 m, 0.10 mm d_c	60°C(0.25') to 280°C (2.52') @ 15.89°/min t_A= 12.37 min; t_A % reduction: 25.6%	P_M = 2s pulse time: 150 ms
Set-up #1b	DB1 10 m × 0.10 mm d_c x 0.10 µm d_f He @ 0.27 mL/min - constant flow Initial head-pressure (p_i relative) 288.54 kPa Outlet pressure (p_{aux} absolute) 253 kPa Hold-up 0.83 min - Outlet velocity 19.95 cm/s	OV17 2.5 m × 0.25 mm d_c x 0.25 µm d_f He @ 11.0 mL/min - constant flow Initial head-pressure (p_{aux} relative) 151.94 kPa Hold-up 2.58 sec - Outlet velocity 225.65 cm/s	MS/FID split ratio 70:30 to MS: 0.5 m, 0.10 mm d_c to FID: 1.1 m, 0.18 mm d_c bleeding capillary: 5.11 m, 0.10 mm d_c	60°C(0.24') to 280°C (2.37') @ 16.87°/min t_A= 11.67 min; t_A % reduction: 24.1%	P_M = 4s pulse time: 150 ms
Set-up #2a	DB1 10 m × 0.10 mm d_c x 0.40 µm d_f He @ 0.27 mL/min - constant flow Initial head-pressure (p_i relative) 307.9 kPa Outlet pressure (p_{aux} absolute) 278 kPa Hold-up 0.88 min - Outlet velocity 18.95 cm/s	OV17 1.8 m × 0.18 mm d_c x 0.18 µm d_f He @ 8.0 mL/min - constant flow Initial head-pressure (p_{aux} relative) 177 kPa Hold-up 0.6 sec - Outlet velocity 292.57 cm/s	MS/FID split ratio 70:30 to MS: 0.5 m, 0.10 mm d_c to FID: 1.1 m, 0.18 mm d_c bleeding capillary: 6.37 m, 0.10 mm d_c	60°C(1.01') to 280°C (10.08') @ 3.97°/min t_A= 48.80 min; t_A % increase: 100.9%	P_M = 3s pulse time: 150 ms
Set-up #2b	DB1 10 m × 0.10 mm d_c x 0.40 µm d_f He @ 0.27 mL/min - constant flow Initial head-pressure (p_i relative) 291.29 kPa Outlet pressure (p_{aux} absolute) 253 kPa Hold-up 0.83 min - Outlet velocity 20.01 cm/s	OV17 2.5 m × 0.25 mm d_c x 0.25 µm d_f He @ 11.0 mL/min - constant flow Initial head-pressure (p_{aux} relative) 151.94 kPa Hold-up 2.58 sec - Outlet velocity 225.65 cm/s	MS/FID split ratio 70:30 to MS: 0.5 m, 0.10 mm d_c to FID: 1.1 m, 0.18 mm d_c bleeding capillary: 5.11 m, 0.10 mm d_c	60°C(0.95') to 280°C (9.5') @ 4.21°/min t_A= 46.05 min; t_A % reduction: 95.2%	P_M = 4.5s pulse time: 150 ms
Set-up #3a	DB1 20 m × 0.18 mm d_c x 0.18 µm d_f He @ 0.5 mL/min - constant flow Initial head-pressure (p_i relative) 227.73 kPa Outlet pressure (p_{aux} absolute) 278 kPa Hold-up 2.72 min - Outlet velocity 13.34 cm/s	OV17 1.8 m × 0.18 mm d_c x 0.18 µm d_f He @ 8.0 mL/min - constant flow Initial head-pressure (p_{aux} relative) 177 kPa Hold-up 0.6 sec - Outlet velocity 292.57 cm/s	MS/FID split ratio 70:30 to MS: 0.5 m, 0.10 mm d_c to FID: 1.1 m, 0.18 mm d_c bleeding capillary: 6.06 m, 0.10 mm d_c	60°C(0.77') to 280°C (7.74') @ 5.17°/min t_A= 37.85 min; t_A % reduction: 78.3%	P_M = 3s pulse time: 150 ms
Set-up #3b	DB1 20 m × 0.18 mm d_c x 0.18 µm d_f He @ 0.5 mL/min - constant flow Initial head-pressure (p_i relative) 207.12 kPa Outlet pressure (p_{aux} absolute) 253 kPa Hold-up 2.52 min - Outlet velocity 13.21 cm/s	OV17 2.5 m × 0.25 mm d_c x 0.25 µm d_f He @ 11.0 mL/min - constant flow Initial head-pressure (p_{aux} relative) 151.94 kPa Hold-up 2.58 sec - Outlet velocity 225.65 cm/s	MS/FID split ratio 70:30 to MS: 0.5 m, 0.10 mm d_c to FID: 1.1 m, 0.18 mm d_c bleeding capillary: 2.76 m, 0.10 mm d_c	60°C(0.72') to 280°C (7.16') @ 5.58°/min t_A= 34.95 min; t_A % reduction: 72.3%	P_M = 4.5s pulse time: 150 ms

Figure 1

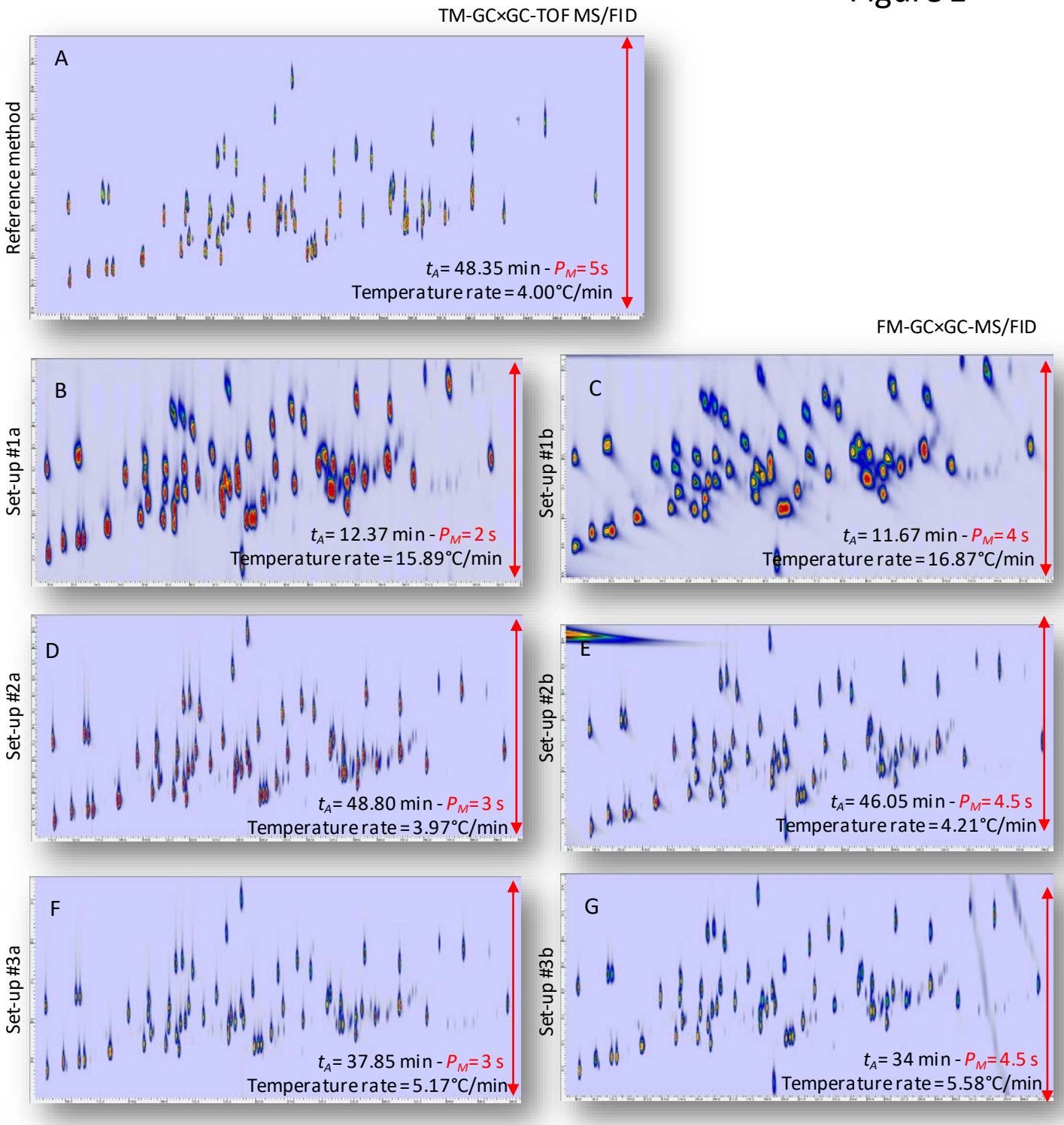
TM-GC×GC-TOF MS/FID
Reference method
A
t_A= 48.35 min - P_M= 5s
Temperature rate = 4.00°C/min
FM-GC×GC-MS/FID
Set-up #1a
B
t_A= 12.37 min - P_M= 2 s
Temperature rate = 15.89°C/min
Set-up #1b
C
t_A= 11.67 min - P_M= 4 s
Temperature rate = 16.87°C/min
Set-up #2a
D
t_A= 48.80 min - P_M= 3 s
Temperature rate = 3.97°C/min
Set-up #2b
E
t_A= 46.05 min - P_M= 4.5 s
Temperature rate = 4.21°C/min
Set-up #3a
F
t_A= 37.85 min - P_M= 3 s
Temperature rate = 5.17°C/min
Set-up #3b
G
t_A= 34 min - P_M= 4.5 s
Temperature rate = 5.58°C/min

Figure 2

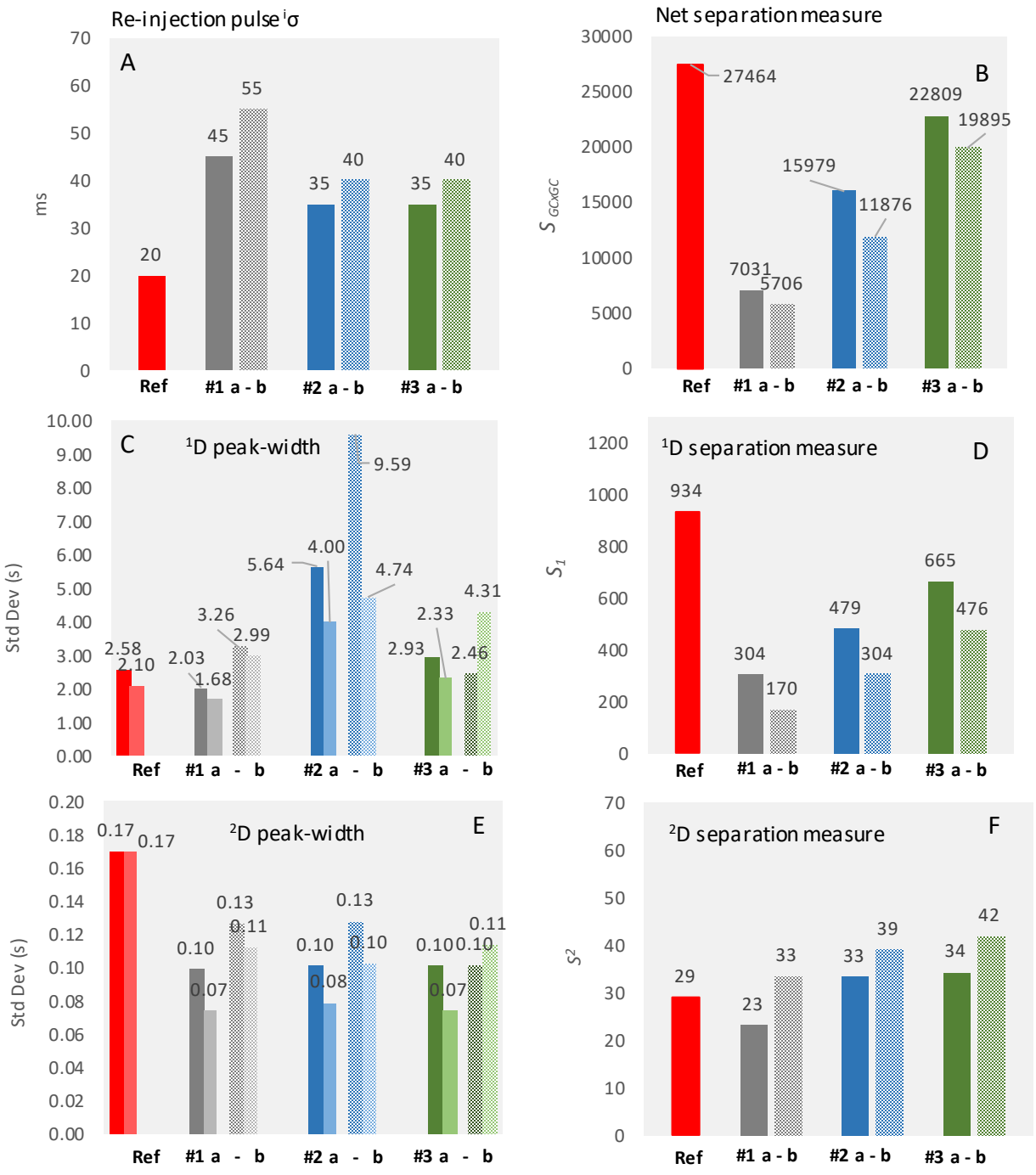
Re-injection pulse σ
A
ms
70
60
50
40
30
20
10
0
20
45
55
35
40
35
40
Ref
#1 a - b
#2 a - b
#3 a - b
Net separation measure
B
S_{GCxGC}
30000
25000
20000
15000
10000
5000
0
27464
7031
5706
15979
11876
22809
19895
Ref
#1 a - b
#2 a - b
#3 a - b
C
¹D peak-width
Std Dev (s)
10.00
9.00
8.00
7.00
6.00
5.00
4.00
3.00
2.00
1.00
0.00
2.58
2.10
2.03
1.68
3.26
2.99
5.64
4.00
9.59
4.74
2.93
2.33
2.46
4.31
Ref
#1 a - b
#2 a - b
#3 a - b
D
¹D separation measure
S_1
1200
1000
800
600
400
200
0
934
304
170
479
304
665
476
Ref
#1 a - b
#2 a - b
#3 a - b
E
²D peak-width
Std Dev (s)
0.20
0.18
0.16
0.14
0.12
0.10
0.08
0.06
0.04
0.02
0.00
0.17
0.17
0.10
0.07
0.13
0.11
0.10
0.08
0.13
0.10
0.10
0.07
0.11
0.10
Ref
#1 a - b
#2 a - b
#3 a - b
F
²D separation measure
S^2
70
60
50
40
30
20
10
0
29
23
33
33
39
34
42
Ref
#1 a - b
#2 a - b
#3 a - b

Figure 3

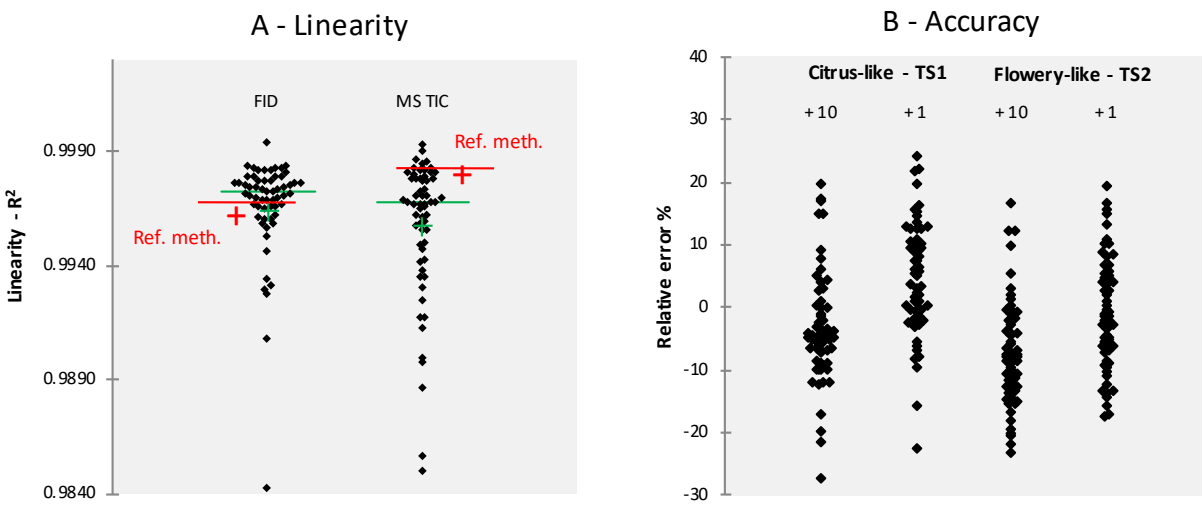
A - Linearity
FID
MS TIC
Ref. meth.
Ref. meth.
Linearity - R²
0.9990
0.9940
0.9890
0.9840
B - Accuracy
Citrus-like - TS1
Flowery-like - TS2
+10
+1
+10
+1
Relative error %
40
30
20
10
0
-10
-20
-30

Figure 4

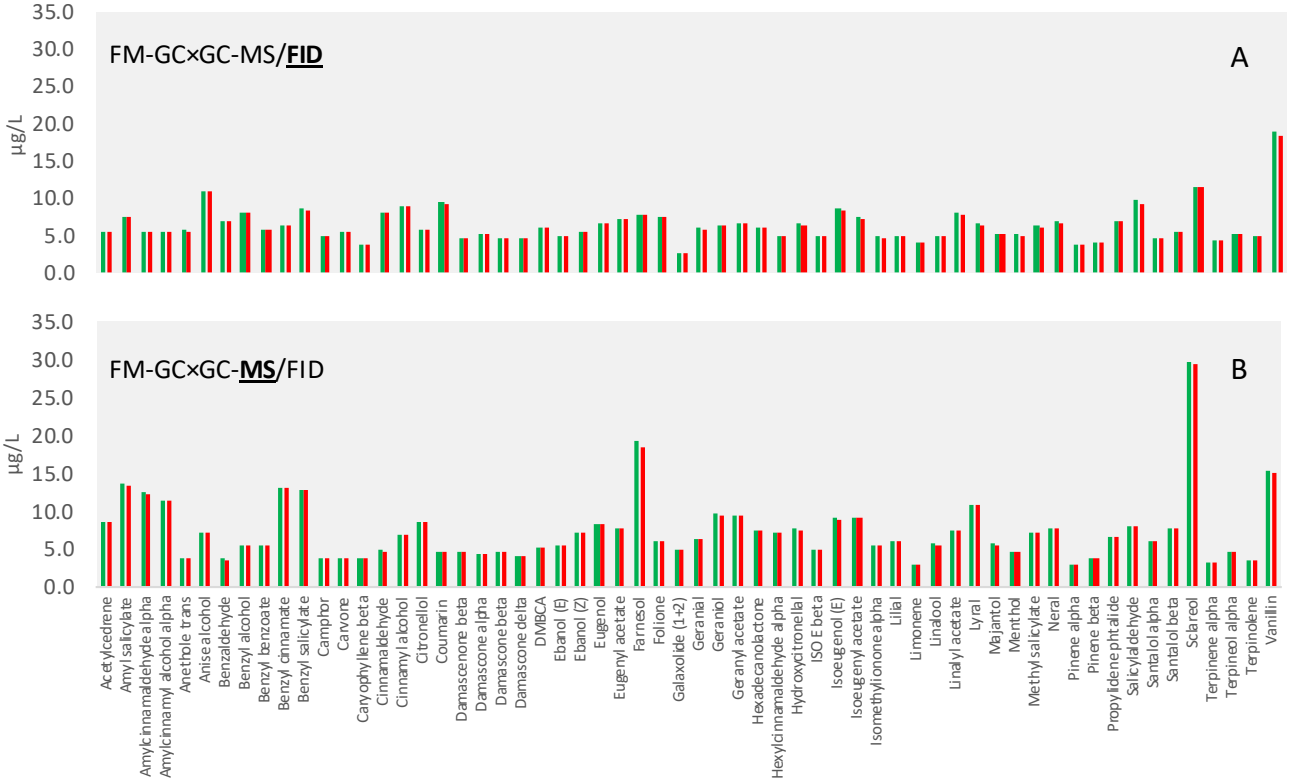
FM-GC×GC-MS/FID
A
µg/L
35.0
30.0
25.0
20.0
15.0
10.0
5.0
0.0
FM-GC×GC-MS/FID
B
µg/L
Acetylcedrene
Amyl salicylate
Amylcinnamaldehyde alpha
Amylcinnamyl alcohol alpha
Anethole trans
Anise alcohol
Benzaldehyde
Benzyl alcohol
Benzyl benzoate
Benzyl cinnamate
Benzyl salicylate
Camphor
Carvone
Caryophyllene beta
Cinnamaldehyde
Cinnamyl alcohol
Citronellol
Coumarin
Damascenone beta
Damascone alpha
Damascone beta
Damascone delta
DMBCA
Ebanol (E)
Ebanol (Z)
Eugenol
Eugenyl acetate
Farnesol
Folione
Galaxolide (1+2)
Geranial
Geraniol
Geranyl acetate
Hexadecanolactone
Hexylcinnamaldehyde alpha
Hydroxycitronellal
ISO E beta
Isoeugenol (E)
Isoeugenyl acetate
Isomethylionone alpha
Lilial
Limonene
Linalool
Linalyl acetate
Lyral
Majantol
Menthol
Methyl salicylate
Neral
Pinene alpha
Pinene beta
Propylidene phthalide
Salicylaldehyde
Santalol alpha
Santalol beta
Sclareol
Terpinene alpha
Terpineol alpha
Terpinolene
Vanillin

Supplementary Material

A step forward in the equivalence between thermal and differential-flow modulated comprehensive two-dimensional gas chromatography methods

Chiara Cordero[1*], Federico Stilo[1], Elena Gabetti[1], Carlo Bicchi[1], Andrea Carretta[2], Daniela Peroni[2], Stephen E. Reichenbach[3,4], James Mc Curry[5]

Authors' affiliation:

1 Università degli Studi di Torino Turin - Italy E-M@il: chiara.cordero@unito.it

2. SRA Intruments SpA, Cernusco sul Naviglio, Milan, Italy

3. University of Nebraska-Lincoln, NE USA

4. GC Image LLC, Lincoln, NE USA

5. Agilent Technologies, Gas Phase Separations Division, Wilmington DE, USA

* Address for correspondence:

Prof. Dr. Chiara Cordero - Dipartimento di Scienza e Tecnologia del Farmaco, Università di Torino, Via Pietro Giuria 9, I-10125 Torino, Italy – e-mail: chiara.cordero@unito.it ; phone: +39 011 6702197

Figure SF1: schematic diagram of the differential-flow modulator implementing the reverse fill/flush (RFF) dynamics.

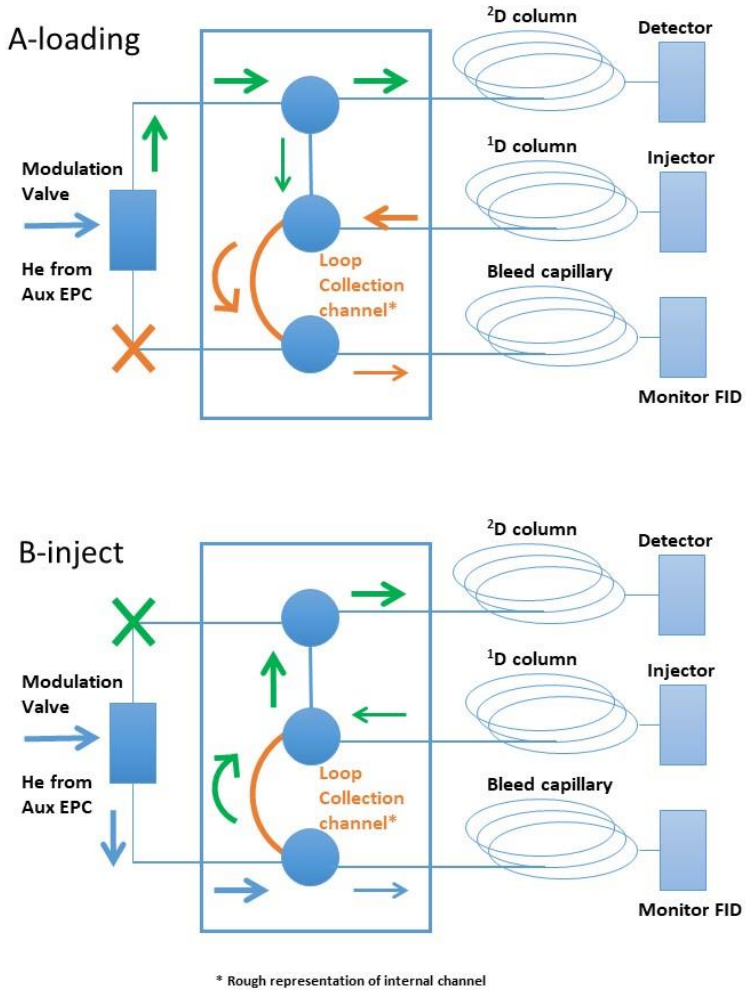

Analytes separated by the ^{1}D column enter at the center port of the modulator plate (^{1}D column in) and fill the fixed size collection channel, which is connected to a bleeding capillary port (bottom port). The length and diameter of the bleeding capillary are chosen according to the pressure/flow conditions of the columns to provide a minimal flow increase of about 10% to the output of the first column [1].

After loading the collection channel, the three-way solenoid micro-valve switches EPC module flow to the bottom post, the channel is flushed, typically for 0.10-0.20 seconds, in the reverse direction of the fill flow into the ^{2}D column at a suitable volumetric flow. The band enters into the ^{2}D columns and undergoes separation in a few seconds. The modulation cycle is then repeated.

[1] M. Giardina, J.D. McCurry, P. Cardinael, G. Semard-Jousset, C. Cordero, C. Bicchi, Development and validation of a pneumatic model for the reversed-flow differential flow modulator for comprehensive two-dimensional gas chromatography, J. Chromatogr. A. 1577 (2018) 72–81. doi:10.1016/j.chroma.2018.09.022.

Figure SF2: step-by-step procedure for chromatographic parameters translation from TM-GC×GC to FM-GC×GC.

Step-1 Reference method TM-GC×GC
Calculation of initial head-pressure (p_i) and mid-point pressure (p_{mid}) at the junction of the two columns - use oven programming initial temperature as reference temp.

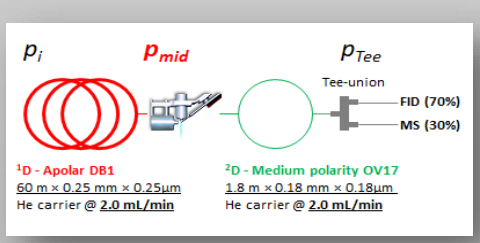

Step-2 Translated method FM-GC×GC
Calculation of initial head-pressure (p_i) and auxiliary carrier pressure (p_{aux}) at the modulator port feeding the ²D column. Pay attention to flow restrictions to avoid loop collection channel overloading.

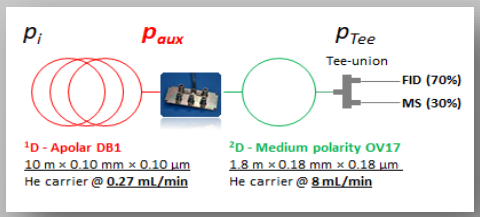

Step-3 Translatable parameters calculation by method translation software
Column dimensions (blue box), initial head-pressures (p_i) and mid-point pressure (p_{mid}) or auxiliary carrier pressure (p_{aux}) at the modulator port are inputted in the dialog box. Reference method temperature programming (yellow box) is inputted in the corresponding dialog box. The model calculates the normalized temperature programming to be used (green dotted-line box).

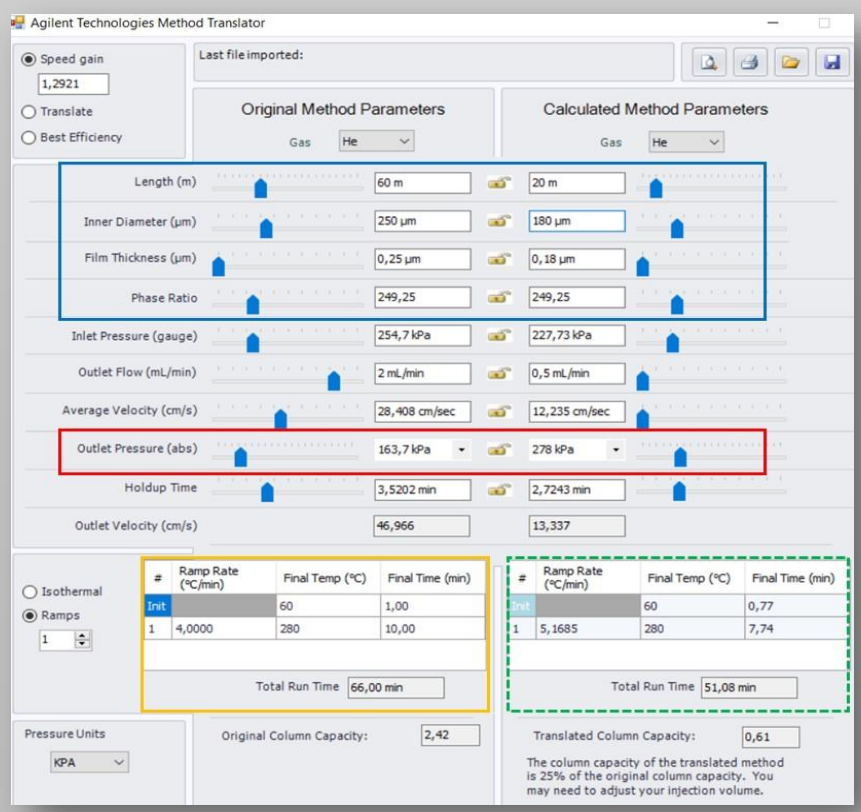

(https://www.agilent.com/en/support/gas-chromatography/gcmethodtranslation)

Figure SF3: relative retention (RR) calculated for the two chromatographic dimensions and taking as reference centroid methyl salicylate and sclareol as last eluting peak. In the ^{2}D the relative retention is normalized to P_M. RR reference equations:

$^1D\ RR = (^1D\ Rt_i - {}^1D\ Rt_{methyl\ salicylate})/{}^1D\ Rt_{sclareol}$

$^2D\ RR = (^2D\ Rt_i - {}^2D\ Rt_{methyl\ salicylate})/P_M$

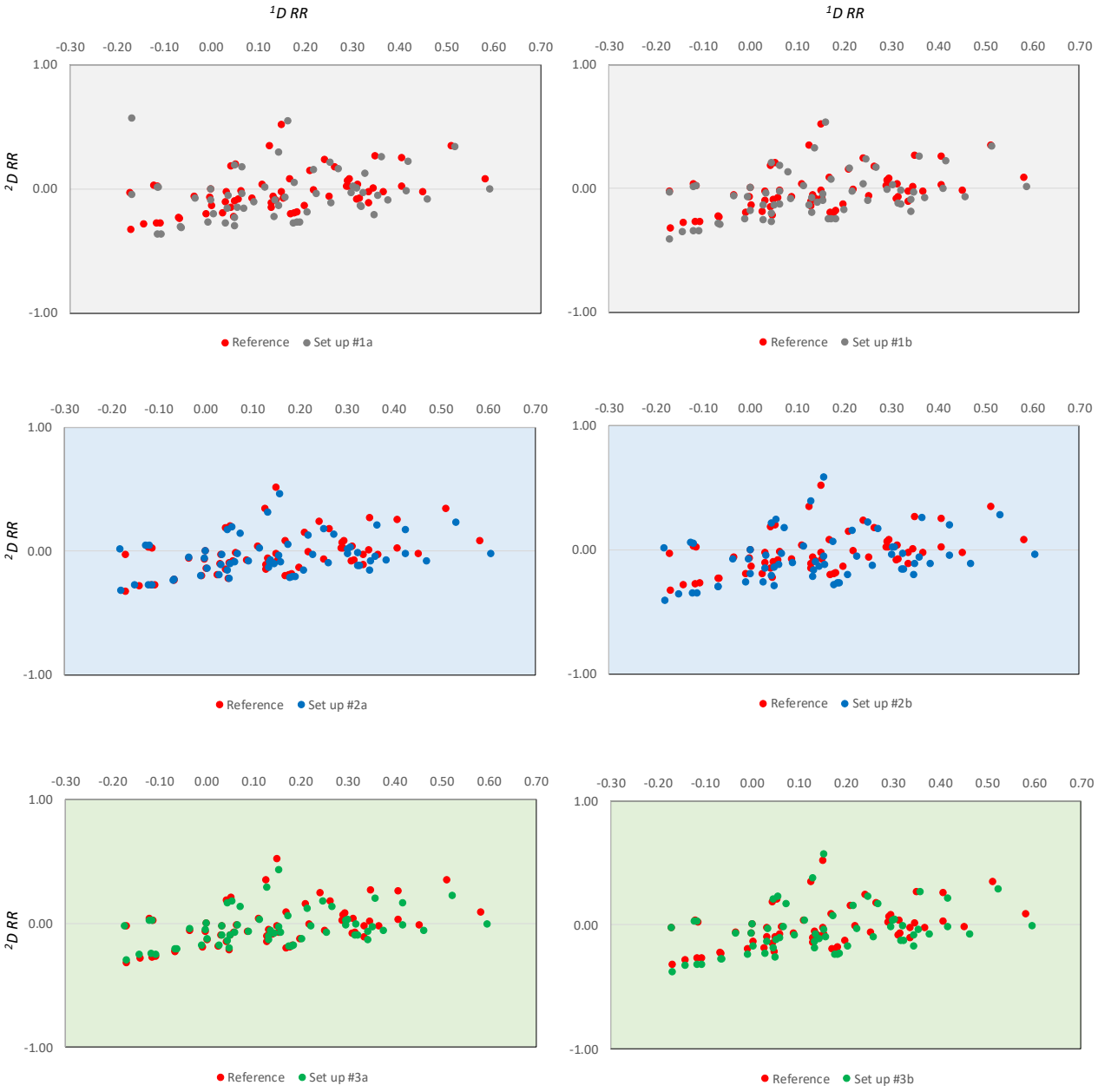

Figure SF4: contour plots of the tested raw fragrance materials (dilution 20% w/v). *Citrus-like* sample TS1 (**A**) and spiked at 1 mg/L level (**B**). *Flowery-like* sample TS2 (**D**) and spiked at 1 mg/L level (**E**). Enlarged areas in **C** and **D** show in higher detail some elution regions on the 2D patterns.

Analyses were by translated method conditions including a ^{1}D DB1 20 m × 0.18 mm d_c x 0.18 µm d_f and a ^{2}D OV17 1.8 m × 0.18 mm d_c x 0.18 µm d_f.

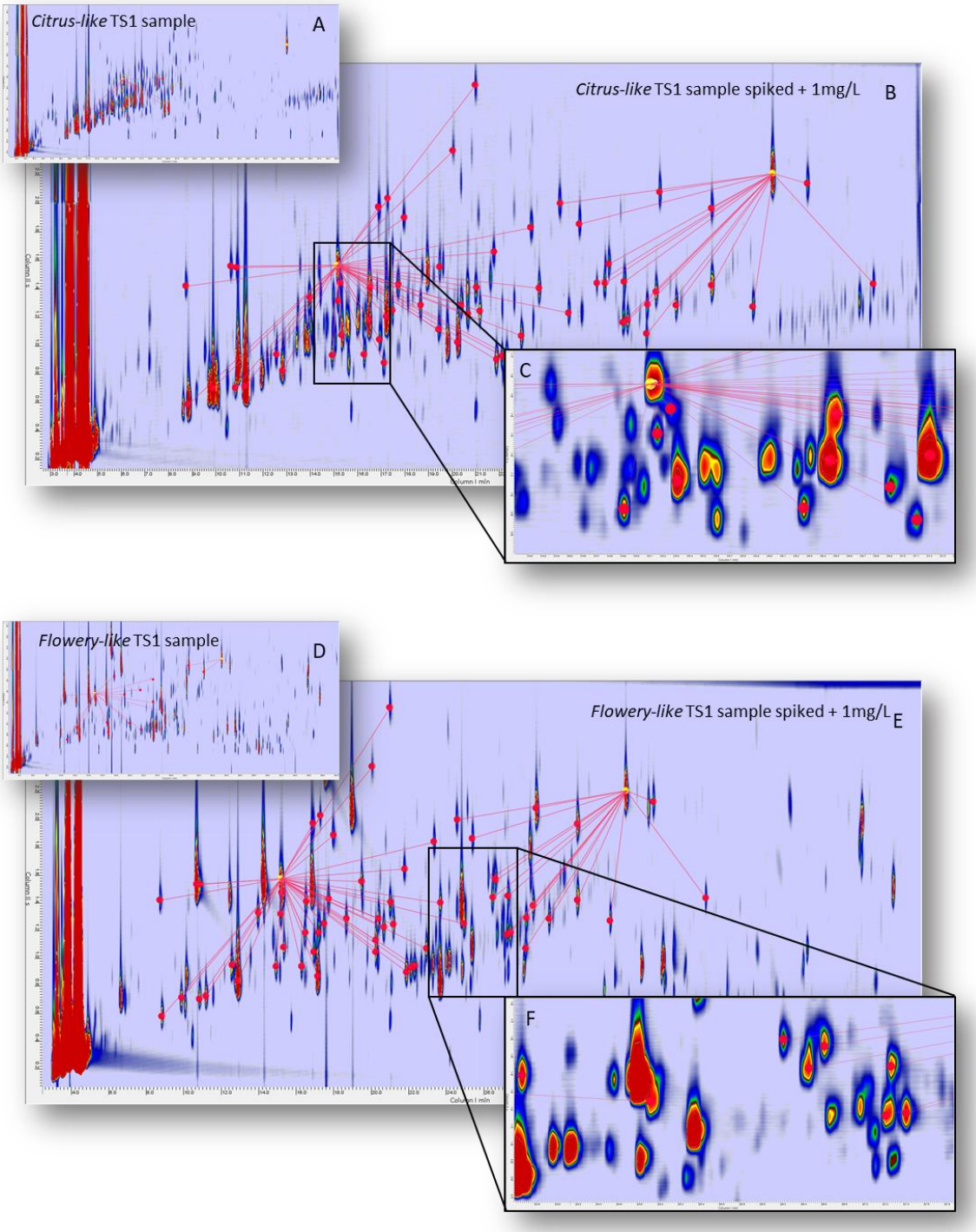

Supplementary Table 1: list of analytes included in the MMix together with peak-widths expressed ad standard deviation (σ) for all tested set ups. Retention times (^1t_R and ^2t_R) are reported for Reference TM and Set up #3a. A graphical visualization of the coherent relative retention between the two configurations is visualized in Supplementary Figure SF3.

	Chromatographic performance – Peak standard deviation σ														Pattern coherence - t_R			
	Reference TM		Set up #1b		Set up #1b		Set up #2a		Set up #2b		Set up #3a		Set up #3b		Reference TM		Set up #3a	
Compound Name	^{1}σ sec	^{2}σ sec	^{1}σ sec	^{2}σ sec	^{1}σ sec	^{2}σ sec	^{1}σ sec	^{2}σ sec	^{1}σ sec	^{2}σ sec	^{1}σ sec	^{2}σ sec	^{1}σ sec	^{2}σ sec	^1t_R min	^2t_R sec	^1t_R min	^2t_R sec
Acetylcedrene	2.94	0.17	2.25	0.07	3.19	0.11	2.55	0.07	2.47	0.10	1.79	0.08	2.68	0.09	37.92	1.96	29.50	1.07
Amyl salicylate	3.66	0.35	1.77	0.07	2.91	0.11	4.20	0.08	4.65	0.09	2.10	0.08	3.00	0.09	32.33	1.77	24.95	1.03
Anethole trans	2.87	0.13	1.68	0.06	2.44	0.09	5.18	0.08	6.59	0.10	2.39	0.10	2.63	0.10	23.25	2.00	17.75	1.21
Anise alcohol	4.11	0.19	2.41	0.05	2.45	0.10	4.61	0.14	5.83	0.15	3.16	0.11	3.59	0.12	22.75	3.10	17.35	1.79
Benzaldehyde	2.58	0.17	2.03	0.10	3.26	0.13	5.64	0.10	9.59	0.13	2.93	0.10	2.46	0.10	11.92	1.94	8.70	1.20
Benzyl alcohol	2.32	0.31	1.56	0.10	3.89	0.16	3.09	0.11	3.00	0.12	2.09	0.12	2.10	0.11	14.33	2.24	10.65	1.33
Benzyl benzoate	4.37	0.19	1.55	0.09	3.36	0.15	4.30	0.09	5.74	0.12	2.48	0.09	2.01	0.11	37.08	3.41	28.85	1.87
Benzyl cinnamate	4.06	0.18	1.83	0.10	2.31	0.11	5.10	0.10	5.50	0.13	2.70	0.09	1.91	0.13	44.92	3.81	35.05	1.92
Benzyl salicylate	3.77	0.35	1.39	0.07	3.44	0.15	4.67	0.09	5.78	0.12	2.40	0.09	3.57	0.12	39.83	3.36	31.05	1.75
Camphor	2.62	0.17	1.34	0.08	3.41	0.11	4.24	0.09	5.72	0.11	1.98	0.08	1.30	0.10	18.50	1.79	13.95	1.12
Carvone	2.51	0.16	1.92	0.08	3.05	0.11	4.08	0.09	4.41	0.11	2.44	0.09	2.08	0.10	21.75	1.96	16.50	1.19
Cinnamaldehyde	4.51	0.22	2.28	0.05	2.72	0.13	4.48	0.12	4.46	0.12	2.61	0.12	3.15	0.12	22.25	3.00	16.95	1.75
Cinnamyl alcohol	4.67	0.40	2.40	0.11	3.76	0.16	6.35	0.11	7.94	0.15	4.04	0.13	3.49	0.12	35.25	2.26	18.00	1.66
Citronellol	2.80	0.31	1.63	0.05	2.25	0.07	4.55	0.08	6.36	0.09	2.43	0.09	1.94	0.09	21.42	1.13	16.30	0.72
Coumarin	5.61	0.21	2.25	0.08	2.30	0.13	6.27	0.14	7.76	0.17	4.10	0.13	3.86	0.15	27.42	4.67	21.05	2.56
DMBCA	2.80	0.14	1.27	0.08	3.44	0.07	3.81	0.09	5.49	0.10	2.37	0.08	1.30	0.09	24.42	1.73	18.65	1.06
Ebanol (E isomer)	3.71	0.27	1.39	0.07	3.34	0.06	5.50	0.08	9.51	0.10	2.03	0.08	2.61	0.09	29.00	1.17	22.30	0.71
Ebanol (Z isomer)	3.12	0.18	0.96	0.07	3.34	0.06	2.62	0.08	3.39	0.10	2.03	0.07	2.61	0.09	28.75	1.11	22.10	0.71
Eugenol	3.53	0.45	2.15	0.09	3.64	0.12	4.65	0.09	5.36	0.11	2.64	0.10	2.61	0.10	25.50	2.26	19.50	1.34
Eugenyl acetate	2.69	0.32	1.71	0.07	2.22	0.08	3.26	0.09	6.19	0.12	2.14	0.09	1.30	0.11	30.33	2.84	23.40	1.62
Farnesol	4.33	0.09	1.92	0.05	6.26	0.09	4.27	0.05	7.70	0.08	3.92	0.05	3.04	0.08	36.42	1.53	28.25	0.86
Folione	2.72	0.07	1.89	0.05	3.83	0.09	2.88	0.05	9.35	0.09	2.39	0.05	1.98	0.08	20.08	1.74	15.20	1.11

	Chromatographic performance – Peak standard deviation σ															Pattern coherence - t_R			
	Reference TM		Set up #1b		Set up #1b		Set up #2a		Set up #2b		Set up #3a		Set up #3b			Reference TM		Set up #3a	
Galaxolide (major isomers)	3.85	0.17	1.91	0.07	3.05	0.11	4.78	0.07	7.35	0.11	2.70	0.07	2.90	0.10		39.83	2.21	31.05	1.22
Geranial	2.82	0.14	1.83	0.08	1.43	0.08	3.37	0.09	3.65	0.10	2.41	0.09	2.08	0.09		22.58	1.60	17.20	0.98
Geraniol	2.71	0.13	1.55	0.04	3.32	0.07	3.63	0.10	5.84	0.09	3.12	0.09	2.31	0.08		22.25	1.33	16.95	0.83
Geranyl acetate	3.33	0.07	1.49	0.04	3.98	0.07	3.20	0.08	7.81	0.07	2.05	0.04	1.89	0.07		26.42	1.34	20.25	0.87
Hexadecanolactone	4.33	0.27	1.46	0.07	2.86	0.11	4.15	0.07	7.07	0.10	1.88	0.07	3.31	0.11		42.00	1.99	32.75	1.08
Hydroxycitronellal	3.07	0.17	2.10	0.05	4.98	0.11	4.18	0.09	8.44	0.11	2.44	0.09	1.36	0.10		23.00	1.69	17.55	1.03
ISO E Super (major isomers)	3.10	0.08	1.36	0.06	2.18	0.08	2.59	0.06	2.43	0.11	1.70	0.06	1.81	0.08		35.17	1.67	27.25	0.97
Isoeugenol (E)	3.22	0.36	2.17	0.10	4.01	0.12	4.34	0.10	7.49	0.13	2.54	0.09	3.17	0.11		28.33	2.50	21.80	1.43
Isoeugenyl acetate	3.07	0.28	1.90	0.07	3.14	0.12	4.32	0.08	6.83	0.12	2.40	0.08	2.14	0.11		32.92	2.97	25.40	1.65
Isomethylionone alpha	5.84	0.10	1.63	0.08	3.86	0.10	2.92	0.08	5.02	0.09	1.97	0.08	2.07	0.09		29.75	1.43	22.95	0.87
Lilial	3.70	0.20	1.70	0.06	3.26	0.10	4.37	0.08	7.18	0.11	2.23	0.08	1.33	0.10		30.75	2.04	23.70	1.19
Limonene	1.87	0.05	1.39	0.07	5.31	0.10	3.77	0.08	4.76	0.07	2.22	0.08	1.30	0.09		15.00	0.73	11.15	0.51
Linalool	3.53	0.19	0.98	0.07	1.15	0.07	2.09	0.07	8.70	0.10	1.84	0.10	1.30	0.08		17.00	0.91	12.85	0.64
Linalyl acetate	2.58	0.10	1.65	0.04	6.79	0.09	4.21	0.06	6.41	0.08	2.66	0.05	1.78	0.08		22.50	0.99	17.10	0.65
Lyral (major isomer)	2.85	0.29	2.00	0.08	2.24	0.09	3.92	0.08	2.80	0.10	2.31	0.08	2.26	0.10		34.42	2.49	26.65	1.36
Lyral (minor isomer)	2.34	0.29	1.93	0.09	2.81	0.02	2.86	0.08	5.34	0.11	2.21	0.09	1.77	0.09		34.25	2.41	26.50	1.32
Majantol	3.10	0.34	1.48	0.07	1.77	0.09	2.60	0.08	5.57	0.10	1.84	0.08	2.67	0.10		27.42	1.97	21.05	1.18
Menthol	2.93	0.14	1.89	0.06	4.40	0.09	5.10	0.07	9.55	0.11	2.34	0.07	1.30	0.09		19.75	1.10	14.90	0.72
Methyl salicylate	3.46	0.52	1.94	0.09	2.90	0.10	5.71	0.08	6.30	0.10	2.92	0.10	1.88	0.10		20.17	2.09	15.25	1.27
Neral	2.23	0.09	1.75	0.05	2.54	0.07	3.67	0.05	4.23	0.08	2.21	0.05	1.33	0.08		21.67	1.57	16.50	0.97
Propylidene phtalide	2.93	0.22	1.97	0.09	2.44	0.13	3.82	0.09	6.89	0.12	2.27	0.10	1.47	0.11		31.83	3.29	24.60	1.78
Salicylaldehyde	3.63	0.52	2.34	0.10	1.15	0.11	4.01	0.11	10.79	0.15	3.03	0.11	3.92	0.11		14.67	2.19	10.90	1.33
Sclareol	2.10	0.17	1.68	0.07	2.99	0.11	4.00	0.08	4.74	0.10	2.33	0.07	4.31	0.11		48.33	2.50	37.85	1.23
Terpinolene	1.44	0.04	1.10	0.08	6.00	0.10	5.19	0.09	2.46	0.09	1.80	0.07	2.23	0.09		16.92	0.94	12.75	0.63
Vanillin	3.75	0.26	2.44	0.11	2.90	0.13	5.57	0.11	8.28	0.17	3.61	0.11	2.97	0.13		26.25	3.81	20.10	2.13
α-Amylcinnamaldehyde	2.83	0.08	1.54	0.06	3.48	0.07	3.74	0.05	3.96	0.08	2.32	0.05	2.25	0.08		34.17	2.19	26.45	1.22
α-Amylcinnamyl alcohol	2.83	0.08	1.98	0.09	3.03	0.14	4.41	0.09	6.05	0.11	3.12	0.09	2.50	0.10		34.33	2.20	27.30	1.24
α-Damascone	3.17	0.17	1.41	0.04	3.43	0.08	3.91	0.08	4.93	0.10	2.28	0.08	1.45	0.08		26.92	1.64	20.70	1.02

	Chromatographic performance – Peak standard deviation σ															Pattern coherence - t_R			
	Reference TM		Set up #1b		Set up #1b		Set up #2a		Set up #2b		Set up #3a		Set up #3b			Reference TM		Set up #3a	
α-Hexylcinnamaldehyde	4.64	0.19	2.19	0.08	3.82	0.10	4.02	0.09	4.46	0.10	2.85	0.08	2.32	0.10		36.92	2.13	28.65	1.17
α-Pinene	1.44	0.10	1.36	0.07	7.19	0.10	4.70	0.07	11.28	0.10	2.04	0.08	1.30	0.08		12.00	0.46	8.80	0.38
α-Santalol	3.52	0.12	1.51	0.05	2.42	0.08	3.70	0.06	4.77	0.09	2.58	0.06	1.47	0.11		35.42	1.71	27.45	0.98
α-Terpinene	2.86	0.06	1.14	0.07	1.15	0.04	3.38	0.08	3.20	0.07	2.05	0.08	1.52	0.08		14.58	0.71	10.85	0.53
α-Terpineol	2.08	0.13	1.65	0.05	3.16	0.07	2.56	0.07	3.04	0.08	2.00	0.06	2.78	0.08		20.25	1.40	15.35	0.87
β-Caryophyllene	3.80	0.17	1.32	0.07	6.52	0.09	2.82	0.07	2.61	0.10	2.38	0.07	1.50	0.09		28.42	1.09	21.90	0.71
β-Damascenone	3.58	0.14	2.10	0.06	3.23	0.06	3.27	0.07	3.75	0.10	2.25	0.07	3.74	0.09		26.58	1.80	20.40	1.08
β-Damascone	2.91	0.25	1.73	0.04	4.14	0.06	4.72	0.08	7.50	0.08	1.96	0.09	2.12	0.06		27.58	1.70	21.20	1.03
β-Pinene	2.37	0.13	1.54	0.07	2.03	0.09	3.43	0.07	5.71	0.09	1.63	0.07	2.61	0.08		13.33	0.67	9.85	0.51
β-Santalol	3.75	0.45	2.33	0.05	3.99	0.07	3.85	0.08	7.17	0.11	2.70	0.08	3.07	0.10		36.42	1.96	28.25	1.06
δ-Damascone	2.80	0.14	1.58	0.07	2.96	0.10	4.72	0.07	4.04	0.10	1.92	0.09	3.18	0.09		26.42	1.54	20.25	0.94
Mean	**3.22**	**0.20**	**1.75**	**0.07**	**3.33**	**0.10**	**4.06**	**0.08**	**5.92**	**0.11**	**2.43**	**0.08**	**2.33**	**0.10**					
Median	**3.07**	**0.17**	**1.71**	**0.07**	**3.19**	**0.10**	**4.08**	**0.08**	**5.74**	**0.10**	**2.34**	**0.08**	**2.23**	**0.10**					